University of Udine

Department of Medical and Biological Sciences

PhD course in Biomedical Sciences and Biotechnology (cycle XVIII)

PhD THESIS

THE INTERACTION BETWEEN EMILIN1 AND α4β1 INTEGRIN: MOLECULAR MECHANISMS, COLITIS AND INFLAMMATION-ASSOCIATED COLORECTAL CARCINOGENESIS

PhD Student: Dr. Giulio Sartori
Supervisor: Prof. Alfonso Colombatti

ACADEMIC YEAR 2016/2017

THE INTERACTION BETWEEN EMILIN1 AND α4β1 INTEGRIN: MOLECULAR MECHANISMS, COLITIS AND INFLAMMATION-ASSOCIATED COLORECTAL CARCINOGENESIS

CONTENTS

1) ABSTRACT **PAG. 5**

2) INTRODUCTION **PAG. 6**

2.1) α4β1 INTEGRIN RECEPTOR **PAG. 6**

2.1.1) Main ligands

2.1.2) Therapeutic potential for α4β1 antagonists

2.2) THE EMILIN/MULTIMERIN FAMILY OF PROTEINS **PAG. 9**

2.2.1) gC1q domain of EMILIN1

2.3) INTERACTION OF gC1q WITH α4β1 INTEGRIN **PAG. 11**

2.3.1) Functional Consequences of the gC1q/Integrin Ligation

2.4) EMILIN1 MOUSE MODELS **PAG. 14**

2.4.1) EMILIN1 in lymphatic vessel function

2.4.2) EMILIN1 in skin homeostasis

2.5) INFLAMMATION-ASSOCIATED COLORECTAL CANCER **PAG. 15**

2.5.1) α4β1 and EMILIN1 expression in human colon cancer

3) AIM OF THE STUDY **PAG. 17**

4) RESULTS **PAG. 18**

4.1) STUDY OF THE AUTOCRINE INTERACTION IN FIBROBLASTS CELLS **PAG. 18**

4.2) STUDY OF THE PARACRINE INTERACTION IN EPITHELIAL CELLS **PAG. 20**

4.2.1) Selection of *in vitro* model

4.2.2) Cells stably transfected with the α4 WT or the mutated integrin chain show the same adhesion but different spreading

4.2.3) Cells stably transfected with the α4 WT or the mutated integrin chain show different proliferative capability

4.3) EMILIN1 SILENCES THE RAS-ERK PATHWAY VIA α4β1 INTEGRIN **PAG. 27**

4.3.1) Downstream effects of persistent cell adhesion to gC1q

4.3.2) The HRas-ERK1/2 pathway is inactivated via the α4 integrin chain

4.3.3) The gC1q ligated α4 integrin chain is physically linked to Hras

4.4) α4β1 AND EMILIN1 EXPRESSION HUMAN COLON **PAG. 31**

4.5) THE E933A TRANSGENIC MOUSE MODEL **PAG. 31**

4.5.1) EMILIN1 E933A transgenic mice present an hyperproliferative phenotype in colon

4.5.2) EMILIN1 WT and E933A newborn isolated mouse fibroblasts show altered proliferation

4.6) DSS-INDUCED EXPERIMENTAL COLITIS **PAG. 35**

4.7) TWO-STEP COLON CARCINOGENESIS (AOM-DSS) **PAG. 41**

4.8) MURINE COLON LEUKOCYTE GLOBAL IMMUNE PHENOTYPE ANALYSIS **PAG. 43**

5) DISCUSSION **PAG. 45**

6) MATERIAL AND METHODS **PAG. 49**

6.1) ANTIBODIES AND OTHER REAGENTS **PAG. 49**

6.2) CELL CULTURES **PAG. 49**

6.3) DNA CONSTRUCTS FOR *EMILIN1* AND *ITGA4* **PAG. 50**

6.4) LIPOFECTION OF SK-LMS-1, HT29 AND SW480 **PAG. 50**

6.5) IMMUNOFLUORESCENCE STAINING OF CELLS FOR EMILIN1 AND KI-67 **PAG. 51**

6.6) PREPARATION OF EXTRACELLULAR MATRIX EXTRACT **PAG. 51**

6.7) WESTERN BLOT ANALYSIS **PAG. 51**

6.7.1) HRas pull down assay

6.8) FACS ANALYSIS OF: **PAG. 52**

6.8.1) Integrin expression

6.8.2) Integrin sorting

6.8.3) Leukocytes from mice peripheral blood

6.8.4) Leukocytes from mice colon tissue

6.9) PLATE COATING **PAG. 54**
6.10) CELL ADHESION (CAFCA) ASSAY **PAG. 54**
6.11) CELL-ELECTRODE IMPEDANCE, REAL-TIME CELLULAR ANALYSIS **PAG. 55**
6.11.1) The adhesion assay
6.11.2) The proliferation assay
6.12) SOFT AGAR COLONY FORMATION ASSAY **PAG. 56**
6.13) IMMUNOFLUORESCENCE STAINING OF TISSUE **PAG. 56**
6.14) GENOTYPING OF TRANSGENIC MICE **PAG. 56**
6.15) FIBROBLAST CULTURES ISOLATION **PAG. 57**
6.16) TREATMENTS *IN VIVO* **PAG. 57**
6.16.1) DSS induced experimental colitis
6.16.2) Two step-colon carcinogenesis model
6.17) HISTOPATOLOGY AND IMMUNOHISTOCHEMISTRY **PAG. 58**
6.17.1) Samples processing
6.17.2) Examination procedures
6.18) ENDOSCOPIC ASSESSMENT OF COLITIS **PAG. 60**

7) REFERENCES **PAG. 61**

8) PUBLICATIONS **PAG. 68**

9) ACKNOWLEDGEMENTS **PAG. 69**

1) ABSTRACT

The interaction between EMILIN1 and α4β1 integrin: molecular mechanisms, colitis and inflammation-associated colorectal carcinogenesis.

The extracellular matrix protein EMILIN1 is the most extensively studied member of the elastin microfibrillar interface proteins (EMILINs) both from the structural and functional point of view. The structure of the gC1q of EMILIN1 solved by NMR highlights unique characteristics compared to other gC1q domains: the residue E933 is the only responsible of the interaction between gC1q and α4β1 and, contrary to integrin occupancy that usually up-regulates cell growth, when gC1q is ligated by the integrin the cells reduce their proliferative activity.

My thesis focuses on this function and, *in vitro*, I demonstrated that EMILIN1 wild type transfected human SK-LMS-1 fibroblasts presented a lower proliferation rate compared to mutant E993A clones. The integrin α4 expressed on fibroblasts interacted with the gC1q and determined a reduced proliferation. Furthermore the gC1q domain exerted an anti-proliferative activity also for α4 transfected colon cancer derived cells.

I planned a DSS induced colitis experiment and a two steps colon carcinogenesis model (AOM plus DSS) to demonstrate that the lack of the interaction between EMILIN1 and α4 determined an enhanced proliferation also *in vivo* in a transgenic mouse where the gC1q domain of EMILIN1 had the E933A mutation, thus not able to interact with α4. I determined the quality and quantity of inflammation in the colitis model, during acute and chronic DSS treatment, and demonstrated that E933A transgenic mice present a much more severe clinical and endoscopic inflammatory disease with a hyper-inflammatory status likely linked to an elevated CD8 T cells although, quite surprisingly, they were much less prone to tumor development compared to wild type littermates.

2) INTRODUCTION

The extracellular matrix (ECM) includes constituents like collagens, elastin, proteoglycans, and glycoproteins that provide a supporting network in which cells exist (Li *et al.* 2007; Zhang and Huang 2011). ECM is a substrate for cell anchorage and serves as a tissue scaffold, but it also elicits profound influences on cell behaviour and affects cell growth, differentiation, motility, and viability (Bissell *et al.* 2005; Marastoni *et al.* 2008; Hynes 2009; Cukierman and Bassi 2010).

The interaction of the ECM to the cells requires transmembrane cell adhesion proteins, the integrins, that are important receptor proteins that translate chemical and physical cues from the ECM into biochemical signals that regulate many interrelated cellular processes (Legate *et al.* 2009). An integrin molecule is composed of two noncovalently associated transmembrane glycoprotein subunits called α and β. The binding of integrins to their ligands produces a variety of downstream signalling events: for instance, integrins activate survival pathways via the PI3K and MAPK pathways and act as essential cofactors for growth factors stimulation (Legate *et al.* 2009; Levental *et al.* 2009; Provenzano and Keely, 2011).

2.1) α4β1 INTEGRIN RECEPTOR

Found on virtually every cell type, integrins are αβ heterodimeric cell membrane receptors which mediate cell interaction with extracellular matrix (ECM). They sense the composition and the mechanical tension within the pericellular milieu, and transmit this information intracellularly to signalling pathways which regulate cell fate by influencing cellular motility, apoptosis, differentiation as well as cell proliferation (**FIGURE 1**) (Moreno-Layseca *et al.* 2014). They are involved in adhesion to ECM components (i.e., Fibronectin, Laminin, Collagens, Vitronectin) but can also participate in certain cell-cell contacts (i.e. Vascular-Cell adhesion molecule, VCAM; Intracellular Cell Adhesion, ICAM) (Petit *et al.* 2000). Integrins recognize aspartic-acid or glutamic-acid based sequence motifs in structurally diverse ligands. Integrin recognition of most ligands is divalent cation dependent and conformationally sensitive (Arnaout *et al.* 2002). There are 18 α subunits and 8 β subunits expressed in various combinations on the surfaces of cells. The integrin superfamily is divided into three families: the Very late Activation (VLA) family (β1), The Leucam family (β2) and the Cytoadhesin family (β3); beta subunits 4-8 are not yet classified into families.

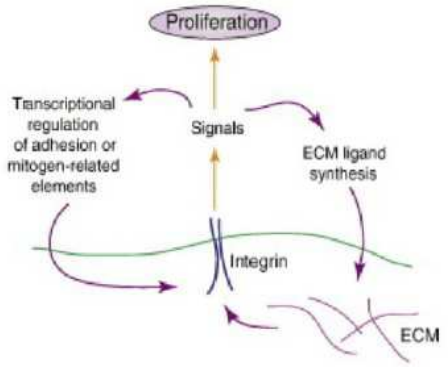

FIG.1) Integrins and extracelluar matrix (ECM) cooperate to sense the composition and the mechanical tension within the pericellular milieu and transmit this information intracellularly to signalling pathways which regulate cell cycle and cell fate, either through physical association or via indirect signalling crosstalk.

The integrin VLA-4 (Very Late Activating Antigen-4, α4β1) is a non covalent heterodimer of the α4 (155 kDa) and β1 (150 kDa) subunits. α4β1 is predominantly expressed on circulating leukocytes and was for a long time consider an exclusive leukocyte integrin, but now there are data available that demonstrates that this integrin is expressed in others normal tissues as well as their tumoral counterparts; α4β1 is expressed i.e. in colon and on many other migratory cell types (i.e.neural crest cells and their derivatives, smooth muscle cells of newly formed blood vessel, epicardial progenitor cells, etc) (Pinco *et al.* 2002; Holzmann et al. 1998). α4β1 binds on activated endothelium primarily to the cell surface immunoglobulin Vascular Cell Adhesion Molecule-1 (VCAM-1) and the CS-1 splice variant of extracellular matrix protein fibronectin (Stephens *et al.* 1999; Clark *et al.* 2000; You *et al.* 2002; Yang *et al.* 2003). Thus, α4β1 and its interactions play important roles during cardiac development, myogenesis, hematopoiesis, lymphopoiesis, immune response (lymphocytes trafficking and activation during inflammation) and embryogenesis. Although an important role for α4β1 in cell migration has been well documented, the precise molecular mechanism that promotes α4β1-dependent cell migration in a complex/focal adhesion independent manner remains to be fully clarified. However, these unusual biological properties seem to depend on the interaction between α4 cytoplasmic domain and paxillin, a signalling adaptor protein (Pinco *et al.* 2002; Hsia *et al.* 2005).

Considered its particularly prominent role in the immune system, it is inevitable the involvement of α4β1 in the pathogenesis of chronic inflammatory diseases such as colitis, asthma, psoriasis allergy, arthritis, atherosclerosis, autoimmune encephalitis and transplant-rejection (Masumoto *et al.* 1992; Yusuf-Makagiansar *et al.* 2002).

2.1.1) Main ligands

α4β1 integrin is a key receptor for several ligands, i.e. VCAM-1, Fibronectin (in particular the HepII/IIICS region), Fibrinogen, Osteopontin, Annexin-1, MAdCAM-1 (Mucosa Addressin Cell Adhesion Molecule), Von Willebrand Factor (VWF), the disintegrinic peptide EC3 and EMILIN1 gC1q Domain. Binding to VCAM-1 is very important due to its tissue localization on the activated endothelium (Hamann *et al.* 1994), the involvement in extravasation phenomena and its potential therapeutic role (Komoriya *et al.* 1991; Makarem *et al.* 1994; Williams and Barclay 1988; Clements *et al.* 1994). The key VCAM-1 binding site is the tripeptide motif sequence IDS. This sequence is homologous to the LDV active motif on the CS-1 peptide of FN, suggesting that α4β1 may interact with FN and VCAM-1 through a similar mechanism.

2.1.2) Therapeutic potential for α4β1 antagonists

Although steroids and other anti-inflammatory drugs with broad-spectrum activities are effective in treating numerous inflammatory diseases, long-term usage is known to have unacceptable side effects, such as greater risk of infection caused by impairment of phagocytic leukocyte migration and function. Therefore, it is desirable to develop drugs that more selectively inhibit specific cellular functions without affecting normal immune surveillance in the treatment of chronic inflammatory disorders. Leukocyte recruitment into the inflamed tissue is an essential physiologic process, however, this beneficial response can also lead to a chronic and detrimental inflammatory process. Since it appears that leukocyte infiltration is a key factor in the pathogenic process of many allergic and inflammatory disorders, finding inhibitors that target α4β1 has been the focus of many pharmaceutical companies. The association of α4β1/VCAM-1 in numerous animal models of human diseases is well documented. The positive clinical results thus far reported for the anti- α4 antibody, Natalizumab, in multiple sclerosis and Crohn's disease confirm an α4β1 role in these diseases (Desilva *et al.* 2008, Conway and Cohen 2010). Also cyclic and linear peptides derivatives that contain the essential binding sequences found in VCAM-1 (IDS) and Fibronectin (LDV) have demonstrated a variety of potent α4β1 antagonistic functions (Wang *et al.* 1995; Yang *et al.* 2003).

In this scenario, and in the light of the high adhesion strength subsisting between EMILIN1 gC1q domain and α4β1, the present studies on the molecular mechanisms of this interaction could contribute to the design of an EMILIN1 gC1q-derived minimal fragment/peptide able to inhibit the α4β1 interaction with various ligands.

2.2) THE EMILIN/MULTIMERIN FAMILY OF PROTEINS

Proteins containing the EMI domain, a sequence of approximately 80 amino acids that includes seven conserved cysteine residues, are members of the ECM EMI-Domain ENdowed (EDEN) family (Braghetta *et al.* 2004). This superfamily comprises seven genes, which can be subdivided into three families on the basis of the major protein domains. The first family is formed by Emu1 and Emu2 genes (Leimeister *et al.* 2002) that except for the presence of an EMI domain do not share structural similarities with the other EDEN members. The second family comprises only one gene EMILIN-truncated (EMILIN-T) with a structure similar to the third larger family, but lacking the C-terminal globular domain of C1q (gC1q). The third is the EMILIN/Multimerin family. The members of this latter family are characterized by the presence of an EMI-domain at the N-terminus, a central part of the molecule is formed by a region of approximately 700 amino acids, with high probability for coiled coil structures presenting heptad repeats. This is followed by a 91-long residue sequence, including two sequences corresponding to structures referred to as the leucine zippers. The finding of leucine zippers is rather unusual especially for an ECM protein as there are very few precedents in the literature reporting the presence of this type of regular spacing of leucines outside the nuclear compartments (Colombatti *et al.* 2000). This region is followed by the coil domain, an interrupted collagenous stalk of 17 GXY triplets. At the end at the C- terminal there is the gC1q domain, a region homologous to the globular domain of the complement (**FIGURE 2**). The EMILIN/Multimerin family includes EMILIN1 (Colombatti *et al.* 1985; Bressan *et al.* 1993; Doliana *et al.* 1999), EMILIN2 (Doliana *et al.* 2001), Multimerin1 (MMRN1; Hayward *et al.* 1991, 1995), and Multimerin2 (MMRN2; Sanz-Moncasi *et al.* 1994; Christian *et al.* 2001).

2.2.1) gC1q domain of EMILIN1

EMILIN1 was originally identified following the attempts to isolate extracellular matrix (ECM) glycoproteins involved in the elastic tissue organization and in the interaction with the surface of elastin producing cells. From the heterogeneous fraction of a newborn chick aorta extract a 115 kDa glycoprotein (gp115) was isolated and subsequently named Elastin Microfibril Interface Located proteIN (EMILIN) for its specific localization at the interface between the amorphous elastin surface and microfibrils (Bressan *et al*, 1993).

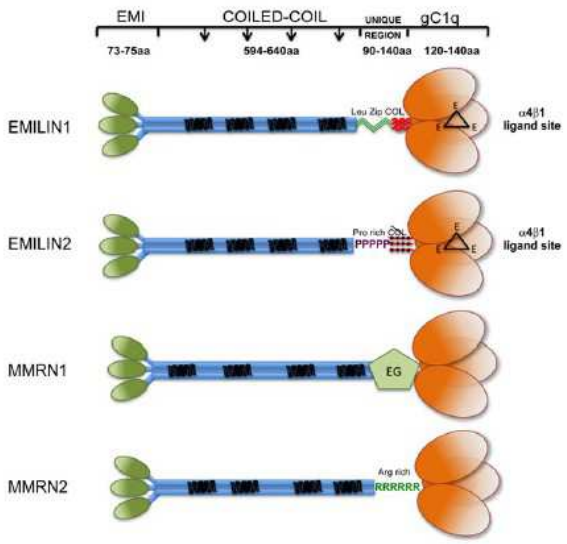

FIG.2) The EMILIN/Multimerin protein family: (EMI) EMI domain; (gC1q) globular C1q-like domain; (COL) collagenous domain; (Pro rich) prolin-rich domain, (Arg rich) arginine-rich domain; (EG) region with partial similarity with EGF domain. The gC1q of EMILIN1 and EMILIN2 possess three unstructured loops (black triangles) each bearing a glutamic acid (E) able to interact with the α4β1 integrin.

The globular C1q (gC1q) domain is a highly conserved structural conformation of approximately 140 residues assembled into trimers. The gC1q domain is part of the C1q/TNF superfamily and it displays very important characteristics (**FIGURE 3**).

The structure of the human EMILIN1 gC1q homotrimer was determine by a three dimensional NMR approach (Verdone *et al.* 2004, 2008, 2009). Three mostly identical gC1q subunits formed the quaternary structure of the complex. The most relevant changes that occur between EMILIN1 gC1q domain and other gC1q (crystal) structures solved to date are the reduction to nine (instead of ten) of the number of antiparallel strands (A,A',B',B,C,D,E,G,H) and the presence of a peculiar unstructured loop spanning from Y927 to G945.

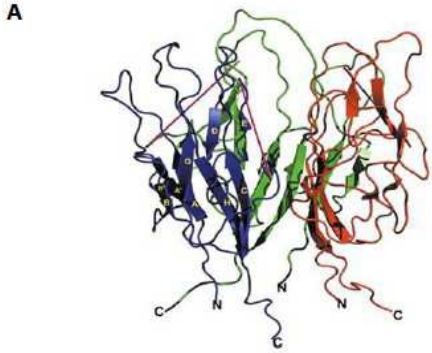

FIG.3) 3D schematic representations of the homotrimeric EMILIN1 gC1q domain: ribbon diagram of the NMR structure is presented; each of three protomers of the trimer are shown in different colours (red, blue, and green). The nine-stranded of each monomer are labeled according to the gC1q/tumor necrosis factor superfamily nomenclature; highlighted in magenta is shown the unstructured segment (Y927-G945) location. B) The strand F (residues in bold) of different members of the C1q superfamily and EMILINs are align. Conserved residues are shaded in gray and the glutamic acid residue interacting whit α4β1 is in yellow.

This sequence is unfolded, highly dynamic and highly accessible to solvent, with 10–11 residues protruding from the main globular structure making this region a good candidate for hosting an interaction site. By site-directed mutagenesis experiments focused on this segment the acidic residue E933 was identified as the site of interaction between gC1q and the α4β1 integrin. Single mutation or even deletion of the loop doesn't affect the gC1q overall domain structure.

The unstructured loop of EMILIN1, that is not present in others already determined gC1q structures, is located at the apex of the homotrimer (**FIGURE 3**) and with the E933 residue is responsible for the interaction with α4β1 integrin; to date this interaction with an integrin is the only one known among gC1q domains.

2.3) INTERACTION OF gC1q WITH α4β1 INTEGRIN

The functions ascribed to the gC1q domain and to the others domain of EMILIN1 are summarize in (**FIGURE 4**) to show the versatility of this glycoprotein (Colombatti *et al.* 2012). EMILIN1 interacts with α4β1 via the globular homotrimeric C-terminus gC1q domain (Spessotto *et al.* 2003, 2006; Verdone *et al.* 2008; Danussi *et al.* 2011).

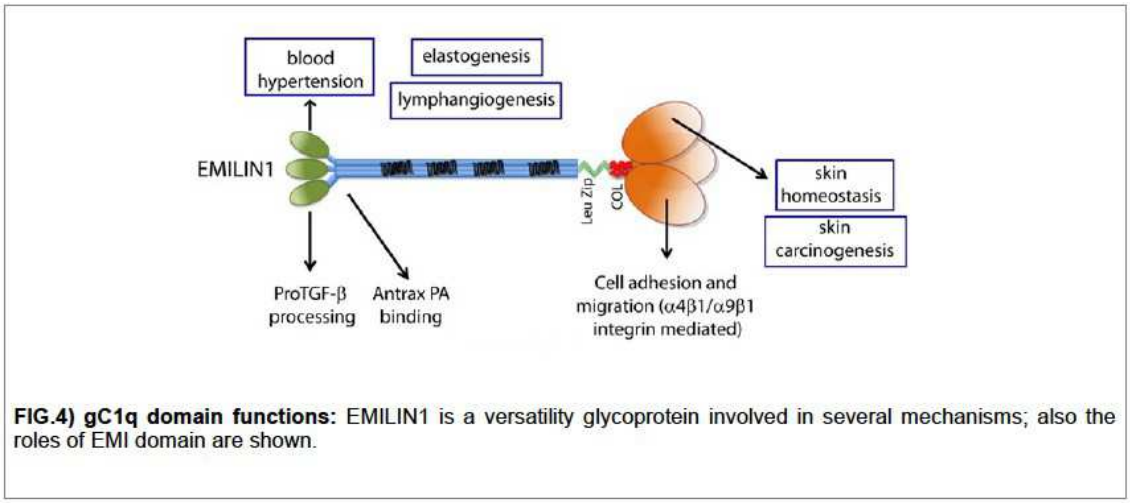

FIG.4) gC1q domain functions: EMILIN1 is a versatility glycoprotein involved in several mechanisms; also the roles of EMI domain are shown.

A common feature to polypeptides with integrin binding capability is the presence of exposed aspartic or glutamic acid residues that are usually placed in protruding loops of the ligand (Leahy *et al.* 1996; Casasnovas *et al.* 1998). These residues are critical for integrin recognition representing the common feature of ECM integrin ligands (Humphries 1990; Humphries *et al.* 2006). The three dimensional conformation of the active site on ligand–receptor binding is extensively demonstrated (in particular for

RGD containing ligands: Humphries 1990; Leahy *et al.* 1996; Arnaout *et al.* 2007; Barczyk *et al.* 2010).

Site-directed mutagenesis experiments in the aspartic acid sequence (e.g., RGD, LDV, KGD, RTD, and KQAGD) and around it showed how these residues are fundamental for integrin recognition: i.e., G in RGD or L in LDV (Pierschbacher and Ruoslahti 1984; Komoriya *et al.* 1991; Cherny *et al.* 1993).

The substitution of a glutamic acid at position 933 (E933) with an alanine residue in the gC1q domain made it no longer functional in cell adhesion assays and it is not recognized by α4β1 integrin. In addition L932A mutant does not loose its cell adhesion binding property and therefore was excluded the possibility that a linear tripeptide from one single monomer as in CS-1 peptide of FN could represent the α4β1 ligand binding site on gC1q. Several others mutant residues around E933 are still functional: in the EMILIN1–α4β1 interaction is not present a short linear peptide consensus sequences and this indicates that the α4β1 integrin binding site involves only a single residue (E933) that seems to play a major role in the interaction gC1q–α4β1 (Verdone *et al.* 2008).

The structure of the human homotrimer EMILIN1 gC1q domain was solved using NMR and revealed the location of residues E933 at the trimer apex in the unstructured loops. The stoichiometry of three integrin molecules for a single gC1q trimer was ruled out for steric reasons. Thus, were proposed two possible patterns of interaction: the involvement of three E933 residues for a single integrin molecule engagement or the need of just one E933 residue for a proper interaction with the integrin. The peculiarity of the gC1q–α4 represents an unique type of interaction and prospects a new model for the interaction geometry recognition between an integrin binding site and a functional ligand located on a homotrimeric assembly (Colombatti *et al.* 2012).

2.3.1) Functional Consequences of the gC1q/Integrin Ligation in Cell Adhesion, Cell Migration and Cell Proliferation.

When EMILIN1 interacts with α4β1 integrin, via the globular homotrimeric gC1q domain, it promotes cell adhesion and migration. Cells attached to EMILIN1 display a pattern of actin and paxillin distribution with accumulation of ruffles-inducing signals and lack of polarization and of stress fiber formation (Spessotto *et al.* 2003). Among the numerous cell types also trophoblast cells could attach with α4β1 integrin to EMILIN1: particularly interesting and rather unexpected they very efficiently migrate toward

EMILIN1 without any prior artificial cellular activation (Spessotto *et al.* 2006).

In contrast to a large body of evidence that signals generated by ligand-activated integrins are in general pro-proliferative (Clark and Brugge 1995; Walker and Assoian 2005; Gilcrease 2007; Streuli 2009), the interaction α4β1 integrin / EMILIN1 downregulates cell proliferation. The finding that EMILIN1 by the direct engagement of the gC1q domain modulates skin cell proliferation points out a novel function of α4β1 (Danussi *et al.* 2011). There is an increase of Ki67 positive cells in epidermis and dermis in *Emilin1*−/− mice, this is accompanied by reduction of PTEN phosphatase and strong up regulation of pErk1/2. The mechanism proposed in **FIGURE 5** show that the presence of EMILIN1 by its gC1q domain and integrin occupancy result in reduced fibroblasts and keratinocytes proliferation by an integrin-dependent increased of PTEN and inhibition of the pEKR1/2 pro-proliferative activity. When gC1q doesn't interact with α4/α9 integrins there is downregulation of PTEN that determined activation of proliferative pathways such as pAkt and pErk1/2. In turn pErk1/2 phosphorylates Smad2 at inhibitory Ser245/250/255 residues and reduces the signalling of TGF-β. Accordingly, targeted inactivation of the *Emilin1* gene *in vivo* induces dermal and epidermal hyperproliferation compared to WT mice where a decreased proliferation of basal keratinocytes and dermal fibroblasts was observed, this scenario seems to be correlated to the downstream changes shown in **FIGURE 5** (Colombatti *et al.* 2012).

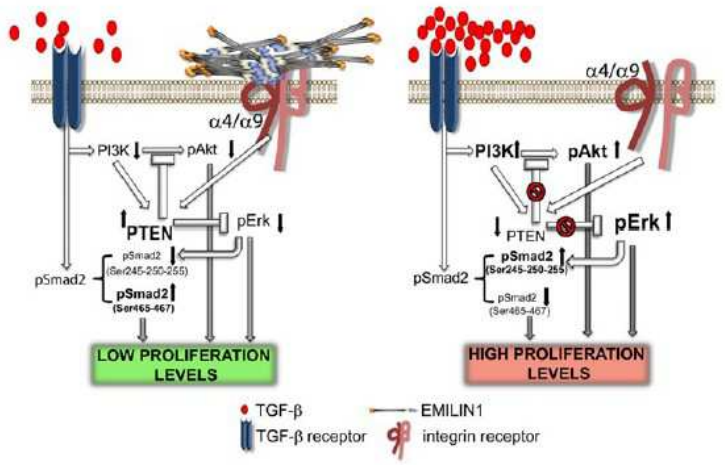

FIG.5) A schematic view of the regulatory role of EMILIN1 in skin: activation of α4β1 integrin (left), mediated by gC1q, determines PTEN activation that inhibits the pro-proliferative activity of pErk1/2. Furthermore TGF-β cytostatic signals are activated via pSmad2 (Ser465/467) and by down-modulation of PI3K/Akt. When EMILIN1 is not present (right) there is a downregulation of PTEN and the activation of the pro-proliferative pAkt and pErk1/2 pathways. In this case, together with TGF-β signalling, there are higher proliferation levels.

2.4) EMILIN1 MOUSE MODELS

The role of EMILIN1 gC1q was further investigated *in vivo*; KO mice were generated and found that the lack of EMILIN1 results: i) in a mild phenotype of lymphatic capillaries (Danussi *et al.* 2008) and vessels (Danussi *et al.* 2013) with increased lymphatic endothelial cell proliferation and ii) in a skin hyper proliferative phenotype (Danussi *et al.* 2011). The last phenotype is strictly dependent on the lack of gC1q.

2.4.1) EMILIN1 in lymphatic vessel function

Targeted inactivation of the *Emilin1* gene in the mouse display no lethal abnormalities (Danussi *et al.* 2008; Zacchigna *et al.* 2006; Zanetti *et al.* 2004) but induces multiple phenotypes characterized by: decreased diameter of arterial vessels and systemic hypertension (Zacchigna *et al.* 2006); structural and functional defects of the lymphatic vessels with a reduction of anchoring filaments (Afs), enlargement of lymphatic capillaries and alterations of the luminal valves of the collectors, with myofibrillar differentiation and proliferation (Danussi *et al.* 2013).

These alterations are associated with inefficient lymph drainage, enhanced lymph leakage, and lymphedema. Notably, this was the first abnormal lymphatic phenotype associated with the deficiency of an ECM protein.

2.4.2) EMILIN1 in skin homeostasis

The skin of mice homozygous for disruption of E*milin1* revealed increased thickness of epidermis and dermis. *Emilin1* interaction with α4β1 (expressed on fibroblasts) provides an antiproliferative signal that seems likely involved in the maintenance of a correct homeostasis between proliferation and differentiation (Danussi *et al.* 2011). This is in sharp contrast with a large body of evidence that signals generated by ligand-activated integrins (Walker *et al.* 2005, Zouq *et al.* 2009), including α4β1 (Boehmler *et al.* 2009), are in general pro-proliferative.

In vitro co-cultures of keratinocytes expressing α4 with wild type EMILIN1- producing fibroblasts inhibits proliferation. The EMILIN1 gC1q domain inhibits cell proliferation through the interaction with the α4 only by “contact” and not by “transwell” (so that the two cell types are physically separated). Proliferative and anti-proliferative signals occur simultaneously and the latter, EMILIN1/gC1q ligation in this case, can override the proproliferative signals only when they reach a certain threshold (Muller *et al.*

2008). The lack of EMILIN1 accelerates tumor development and increases the number and size of skin tumors compared to WT mice in a two-step skin tumor carcinogenesis protocol (Danussi *et al.* 2013). EMILIN1 deficiency in these mice implies the lack of EMILIN1 ligation to α4β1/α9β1 integrins and presented a pro-tumorigenic environment that causes aberrant skin homeostasis.

Functional studies reported PTEN as a critical tumor suppressor for skin cancer in humans and in mice (Di Cristofano *et al.* 1998; Segrelles *et al.* 2002; Suzuki *et al.* 2003) by negatively regulating signal pathways involved in cell proliferation (Schindler *et al.* 2009).

PTEN downregulation was seen in *Emilin1*−/− mice also in the skin tumor environment: it seems likely that the mechanisms controlling the homeostasis of cell proliferation and the enhanced tumor development when EMILIN1 expression is genetically or functionally knocked down depends on the unique mode of gC1q–α4β1/α9β1 integrin interaction (Colombatti *et al.* 2012).

2.5) INFLAMMATION-ASSOCIATED COLORECTAL CANCER

The colitis-associated cancer (CAC) is characterized by poor prognosis and a relatively high mortality rate of ~50%. The persistent cycles of tissue damage and repair lead to molecular events that drive precursors lesions to cancer. In colitis associated cancers, continuous tissue destruction and renewal along with oxidative damage can trigger mutagenesis and cancer initiation (Lakatos *et al.* 2014; Risques *et al.* 2011) so that the competitive benefit of mutations during tumor initiation is dependent on the contextual (i.e. inflammatory) microenvironment in which they arise as shown in a dextran sodium sulphate (DSS) model (Vermeulen *et al.* 2013). Chronic inflammation contributes to tumorigenesis at all stages. It takes part to cancer initiation by generating genotoxic stress, to cancer promotion by inducing cellular proliferation, tissue repair and secretion and deposition of extracellular matrix (ECM) molecules, and to cancer progression by enhancing angiogenesis and tissue invasion (Grivennikov *et al.* 2010). Here, the immune system plays a dual role (Hagerling *et al.* 2014): it can not only suppress tumor growth, but also promote tumor progression, either by selecting for tumor cells that are fit to better survive or by establishing a local immunosuppressive environment, achieved by secretion of immunosuppressive soluble mediators despite systemic immunocompetence (Schreiber *et al.* 2011). These molecules include among others

TGF-β, which suppresses effector NK-cells, DCs and T-cells, IL-10, able to inhibit T cells and VEGF, that leads to increased angiogenesis. Progressing tumors often attract regulatory and suppressive immune cells (Vesely *et al.* 2011).

2.5.1) α4β1 expression in human colon cancer

α4β1 is predominantly expressed on circulating leukocytes and its important role in cell migration has been well documented (Pinco *et al.* 2002; Hsia *et al.* 2005). There are several studies that identified *ITGA4* expression in colon tissue and its methylation in colitis and colon adenomas/carcinomas. Methylated *ITGA4* of tissue is present in 75% of colon adenomas, 92% of colon adenocarcinomas and 6% of colon mucosa (Zhang *et al.* 2015). Methylated *ITGA4* in the fecal sample was found in 69% (9/13) of patients with colon adenomas and in 21% (6/28) of patients with no polyps (Ausch *et al.* 2009). This conditions decreases the expression of *ITGA4* gene expression.

Previous studies have demonstrated that *ITGA4* is hypermethylated also in inflamed colon tissue/colitis (Gerecke *et al.* 2015) and that the treatment with anti-α4 antibodies further aggravate colitis by IL-1β, TNF-α, and IFN-γ producing cells recruitment (Bjursten *et al.* 2005). Conversely, the treatment with α4 antibodies in combination with conventional therapies alleviates colitis by suppression of IL-1β and iNOS in mouse models (Gillberg *et al.* 2013). Since these anti-inflammatory genes are constitutively hypermethylated in tumors of CAC patients, these proteins could potentially drive CAC initiation and progression and thereby serve as targets for pharmaceutical intervention and therapy.

3) AIM OF THE STUDY

It was reported that when EMILIN1 interacts with cells expressing the α4β1 integrin there is a significant downregulation of cell proliferation in a skin model. Colon cancers were among the first tumors in which a functional link between inflammation, tumor microenvironment and cancer progression had been noted. The overall objective of this study was to analyze the mechanisms and the putative functional consequences of the interaction between the extracellular matrix (ECM) protein EMILIN1 and the integrin cell receptor α4β1. I hypothesize that the interaction EMILIN1/α4 could be potentially involved in the regulation of colitis and colon carcinogenesis.

The present study is organized in two main sections:

- In the first section I studied this interaction in *in vitro* experiments with two models: an autocrine system with fibroblasts, in which cells expressing α4β1 deposit EMILIN1 in the ECM, and a paracrine system with epithelial cells, in which α4β1 was transfected to increase its expression. In this latter model EMILIN1 is provided as a recombinant protein substrate. In both models *in vitro* analyses on transfectants cell lines, for EMILIN1 wild type (WT) or mutated and for wild type (WT) or α4 mutated, are presented in order to clarify the functional profile of α4β1-EMILIN1 interaction.

- In the second section the role of this interaction is investigated first in experimental colitis and then in a two-step inflammation-associated colorectal cancer in mice.

My hypothesis is supported by the evidence of a down-regulation of the expression of EMILIN1 and α4 in some human colorectal carcinomas biopsies.

4) RESULTS

4.1) STUDY OF THE AUTOCRINE INTERACTION IN FIBROBLASTS CELLS

It is known that during tumor development there is a derangement of the ECM (Cox *et al.* 2011) that can contribute to the local dissemination of cancer cells and that some integrins (i..e. α5β1 or αvβ3) are important for a proper ECM deposition (Ruoslahti and Pierschbacher 1987; Ruoslahti 1999; Campbell 2008). To assess if also the α4β1 integrin has any specific role in the extracellular deposition and supramolecular organization of EMILIN1, the molecular mechanism and the role of the α4 integrin chain on fibrillar deposition and proliferation was first investigated in human SK-LMS-1 cells. This cell type produces an organized ECM, comprising low levels of EMILIN1, and presents moderately strong α4β1 expression levels providing us an autocrine model to study the consequences of the interaction between EMILIN1 and α4β1. SK-LMS-1 cells were transfected with eukaryotic expression vector pCDNA-3 (hygro) containing the human wild type (WT) EMILIN1 or the E933A mutant sequences (as described under Materials and Methods) to obtain stable transfectant lines. The mutant E933A form was used as a negative control since it has been reported that the E933A gC1q domain is unable to interact with α4β1 (Verdone *et al.* 2008). Semi quantitative evaluation of exogenous protein expression was performed analysing ECM protein extracts by Western Blot (**FIGURE 6A**). I checked that during the experiments the membrane α4 expression was maintained at high levels. The different clones were assessed by FACS analysis and found to be high expressors (**FIGURE 6B**).

Subsequently, I investigated if the interaction between EMILIN1 and the α4β1 integrin was necessary for a proper deposition and fibrillar organization of EMILIN1. Several cell clones were grown on cover-glass slides (for three days) and were stained with AS556 (a polyclonal antibody against human EMILIN1) for immunofluorescence detection. The cellular clones expressing the wild type construct exhibited a complex and well-organized EMILIN1 ECM fibrillar deposition with intermingled fine fibrils throughout the matrix. On the other hand, clones containing the mutated constructs showed altered EMILIN1 fibrillar deposition (**FIGURE 7A**). The EMILIN1 extracellular fibrils appeared short and fragmented with evidence of accumulation in knots and the resulting overall network organization was severely compromised.

FIG.6A

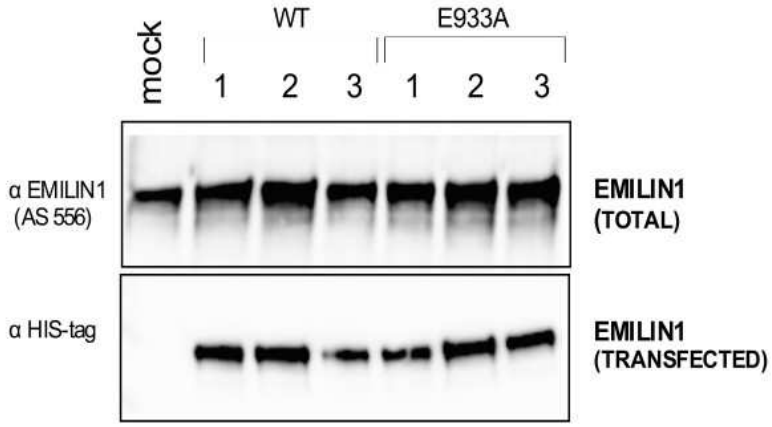

FIG.6B

	WT (1)	WT (2)	WT (3)	E933A (1)	E933A (2)	E933A (3)
2 DAYS	70.00%	90.00%	87.00%	84.00%	83.00%	82.00%
4 DAYS	41.00%	35.00%	26.00%	33.00%	32.00%	30.00%

FIG.6) EMILIN1 and α4 expression in SK-LMS1 transfected cells:
A) EMILIN1 WT and E933A SK-LMS1 transfected cells show increased levels of EMILIN1 expression compared to mock. The increased is due to the HIS-tag EMILIN1. B) FACS analysis reveals the same % of α4 expression on both clones after 2 and 4 days.

Furthermore, the WT transfected cells presented a lower proliferation rate, measured as the percentage of cells that are positive for Ki-67, compared to mutant E993A clones (**FIGURE 7B**).

FIG.7A

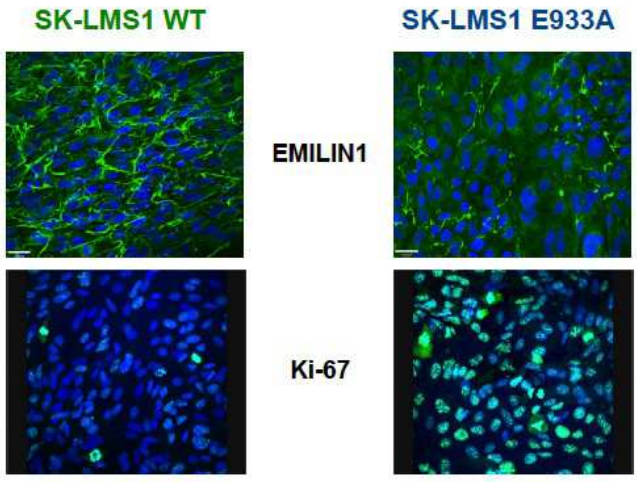

FIG.7B

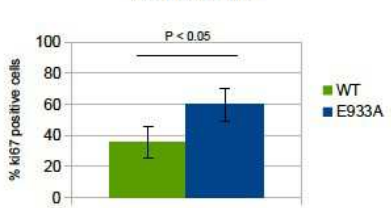

FIG.7) EMILIN1 and Ki67 immunofluorescence analysis:
A) E933A SK-LMS1 transfected cells show compromised extracellular fibrils organization and increased levels of the proliferative marker Ki67 compared to EMILIN1 WT transfected cells. B) Quantification of the % of cells positive to Ki67 after 48h.

These results suggest that the interaction between EMILIN1 and the α4β1 integrin is necessary for a well organized deposition and the lack of this interaction results in deranged EMILIN1 supramolecular organization and higher proliferation rates.

4.2) STUDY OF THE PARACRINE INTERACTION IN EPITHELIAL CELLS

In the above *in vitro* models the cells studied were able to produce and deposit EMILIN1 and they engaged the α4β1 integrin in an autocrine manner. However in most cases, and certainly in epithelial cancers, to investigate the consequences of this interaction a different experimental setting is necessary since epithelial cells do not produce EMILIN1. In epithelial tissues EMILIN1 is synthesized and secreted by fibroblasts and cells that express the appropriate integrin can interact with EMILIN1. In our paracrine model epithelial cells were transfected with α4 integrin chain and EMILIN1 is provided as a recombinant protein substrate.

It is known that α4 is expressed on normal human intestinal epithelial cells (IEC) and it is absent from several colon cancer cell lines (**FIGURE 8**).

FIG.8A

Cell line	Localization	β1	α4
IEC	INTESTINAL EPITHELIAL CELL	Y	Y (20%)

FIG.8B

Cell line	Localization	Duke's type	Grade	β1	α4
SW1116	Primary lesion (CA)	A	III	Y	N
CACO2	Primary lesion (CC)	B	II	nd	N
SW480	Primary lesion (CA)	B	III	Y	N
HT29	Primary lesion (CA)	B	II	Y	N
DLD1	Primary lesion (CA)	C	-	nd	N
SW948	Primary lesion (CA)	C	III	nd	N
HCT116	Primary lesion (CC)	D	-	nd	N
SW620	Lymph node met (CA)	C	III	nd	N
LOVO	Metastatic nodule (CA)	C	IV	nd	N

FIG.8) β1 e α4 FACS analysis A) of intestinal epithelial cells and B) on colon cancer cell lines (Y= yes expressed, N = not expressed, nd= not detected).

For further experiments I selected two colon cancer cell lines, HT29 and SW480, which possess a different membrane expression pattern of integrins as well as different mutation profiles at relevant oncogenes (summarized in **FIGURE 9**).

	HT29	SW480
α1	0%	14%
α2	97%	95%
α3	45%	90%
α4	0%	0%
α5	0%	81%
α6	-	97%
αv	10%	-
PI3KCA		Exon 9
RAS	WT	mutated (codon 12)
P53	mutated (codon 273)	mutated (codon 273)
EGFR	WT	WT
BRAF	mut	WT

FIG.9) Endogenous Integrin expression and gene mutation status panel of HT29 and SW480 colon cancer cell lines.

4.2.1) Selection of *in vitro* model

HT29 AND SW480, were transfected with the eukaryotic expression vector pCDNA-3 (G418) containing, respectively, the *ITGA4* (the α4 integrin chain gene) WT or the *ITGA4* mutant sequences (deprived of the cytoplasmic tail) to obtain stable transfectant lines. The aim here was double: to determine if the expression of the α4 integrin could reduce the proliferation of cancer cells when confronted with EMILIN1; and to test if the cytoplasmic tail of the integrin α4 chain is involved in the anti-proliferative function. The clones selected, each from a different colon cancer cells lines, where tested in a Western Blot analysis with two different antibodies, one for the C-terminal and the other for the N-terminal of the integrin α4 chain.

As expected, both the α4 WT and the α4 mutated chains were recognized in immunoblots of cell extracts by the α4 N-terminal antibody but only the α4 WT clones were recognized also by the C-terminal antibody (**FIGURE 10A**).

I then checked if the integrin α4 chain was present at the cell membrane by FACS analysis. The result underlines a medium level of cell membrane expression; thus, in order to enrich for cells with the highest membrane expression I sorted the positive cells for α4 (**FIGURE 10B**).

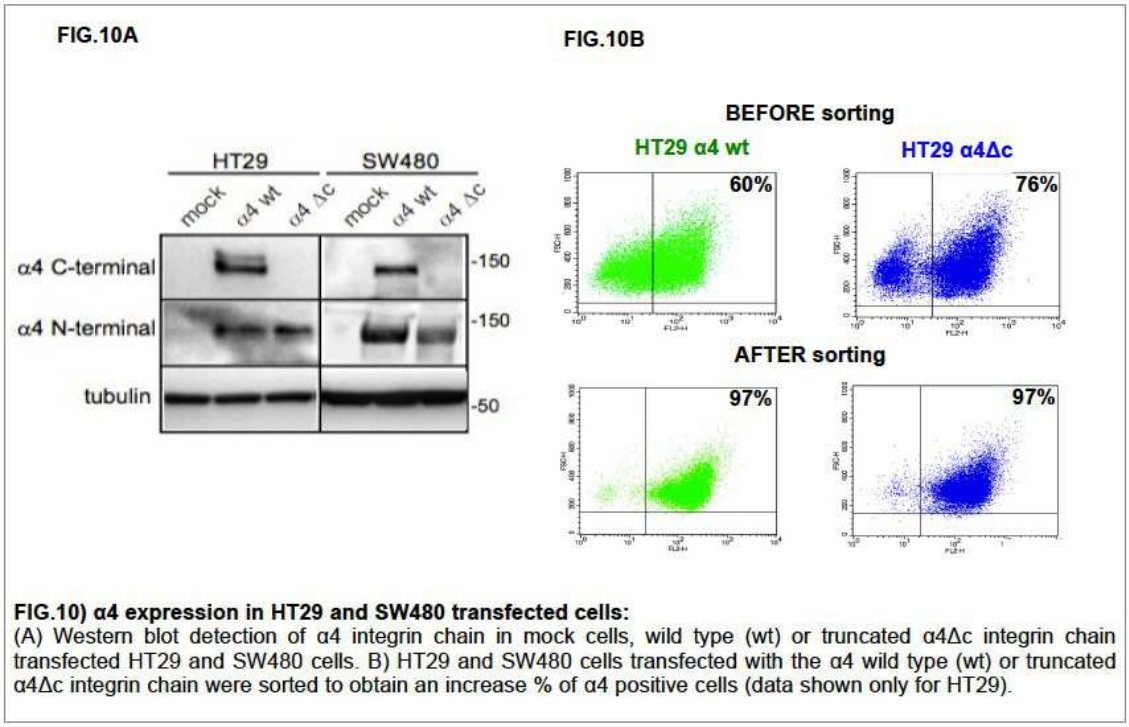

FIG.10) α4 expression in HT29 and SW480 transfected cells:
(A) Western blot detection of α4 integrin chain in mock cells, wild type (wt) or truncated α4Δc integrin chain transfected HT29 and SW480 cells. B) HT29 and SW480 cells transfected with the α4 wild type (wt) or truncated α4Δc integrin chain were sorted to obtain an increase % of α4 positive cells (data shown only for HT29).

4.2.2) Cells stably transfected with the α4 WT or the mutated integrin chain show the same adhesion but different spreading

To check if the transfected integrin α4 chain was able to promote cell adhesion I used the CAFCA assay, a well established assay of our laboratory to measure the percentage of bound cells. The Jurkat cells express high levels of the α4β1 integrin and attach very efficiently to gC1q/EMILIN1. Both HT29 and SW480 cells transfected with either the α4 WT or the α4 mutated chain were able to bind to gC1q/EMILIN1, indicating that the transfected integrin α4 chain was functional (**FIGURE 11**).

However, while the adhesive capability to the gC1q/EMILIN1 ligand of both WT as well as mutated α4 integrin chain were comparable, the spreading onto the substrate, measured in real-time by a cell-electrode impedance assay, was much higher in HT29 and SW480 α4 WT clones compared to the α4 mutated clones. This indicated that the cytoplasmic tail of the α4 integrin chain is involved in the spreading signalling (**FIGURE 12**).

Notably, the same clones on other ligands (ex: FN) had a different behaviour depending on integrins expression on their membrane (**FIGURE 12A**): HT29 mock transfected cells do not spread on FN; on the contrary, SW480 mock transfected cells spread on FN; this different behaviour is due to the presence of the α5 integrin chain in the membrane of these latter cells (**FIGURE 9**).

FIG.11A

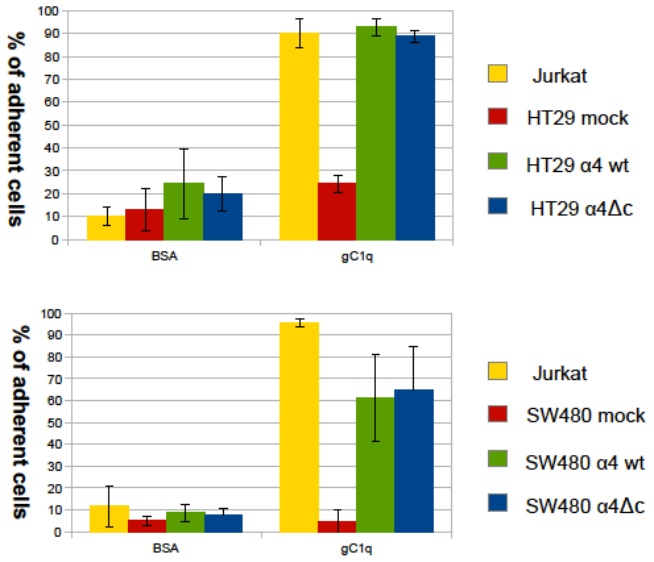

FIG.11) Cells transfected with α4 integrin adhere to gC1q:
A) HT29 and SW480 cells transfected with the wild type (wt) or truncated (Δc) a4 integrin chain were allowed to adhere to gC1q or BSA as control in CAFCA miniplates. Jurkat cell and mock cells were used as positive and negative controls of adhesion respectively.

FIG.12A

FIG.12B

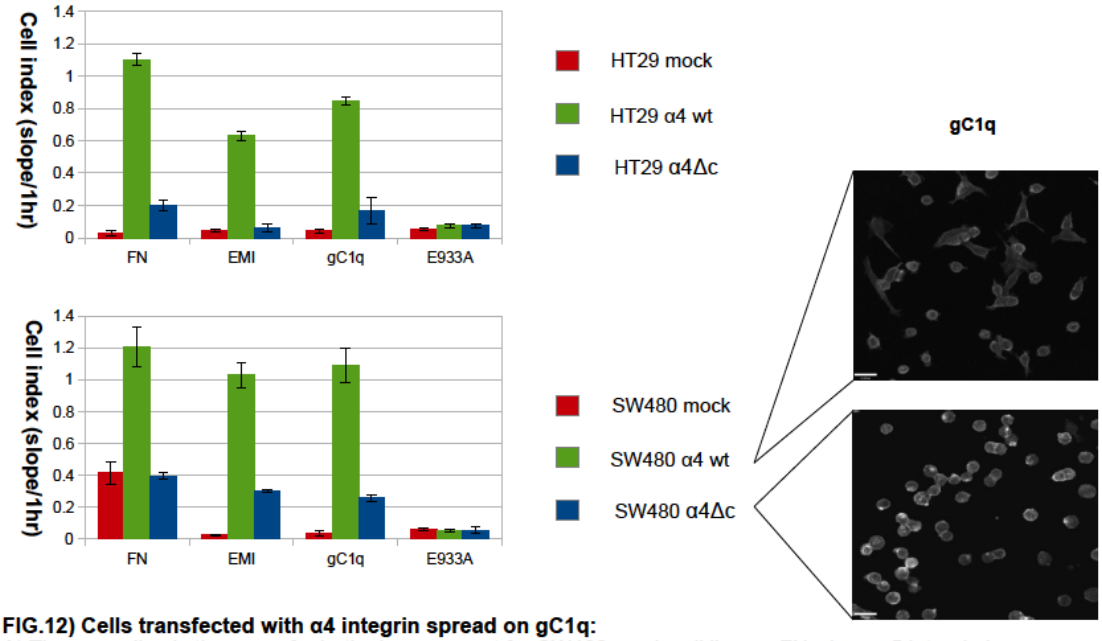

FIG.12) Cells transfected with α4 integrin spread on gC1q:
A) The spreading is the same for both clones except for SW480 mock cell line on FN where α5 integrin is expressed
B) Phalloidin staining for SW480 α4 wt and SW480 α4Δc cell spreading on gC1q

4.2.3) Cells stably transfected with the α4 WT or the mutated integrin chain show different proliferative capability

The proliferation activity was tested with three different approaches: the cell-electrode impedance assay (able to monitor in real-time the cell proliferation), a soft agar colony formation assay and a staining with the Ki-67 antibody.

The same cell-electrode impedance assay used to quantitate cell spreading is able to monitor the proliferation capability if serum is added to the medium. Here, only the cell clones expressing the integrin α4 WT chain interacted with the gC1q/EMILIN1 and underwent increased doubling time compared to the cell clones expressing the mutated integrin α4 chain (FIGURE 13A). The former clones displayed a reduced proliferation rate measured as normalized cell index (data shown only for HT29 clones FIGURE 13B).

In addition I plated HT29 transfected clones in agar in the presence or in absence of gC1q and the colonies of the cells transfected with the wild type α4 integrin chain were significantly less in the presence of gC1q (**FIGURE 13C**); on the contrary the colonies of HT29 transfected with the mutant α4 integrin grew to the same number under all the experimental conditions (**FIGURE 13D**).

The proliferation rate of integrin α4 transfectants colon cancer cell lines was also tested with the Ki-67 assay. The results are expressed as the percentage of cells that are positive for Ki-67, comparing first of all HT29 and SW480 growth on different ligands: Fibronectin and its domain CS-1, EMILIN1 and its domain gC1q and E933A mutated EMILIN1 as negative control. A lower percentage of Ki-67 positive staining (10 – 20 %) was detected for cells growing on EMILIN1 and its domain gC1q compared to other ligands (30 – 50 %) (**FIGURE 14A and 14C**). We also confirmed the reduced percentage of Ki-67 only on gC1q in a time-course experiment at 24, 48 and 72 hours (**FIGURE 14B and 14D**).

All these data confirm that the cytoplasmic tail of the α4 integrin is responsible for the anti-proliferative capability when it interacts with EMILIN1 or its globular gC1q domain.

Furthermore, the E933 residue is of great importance to bind α4 and to allow the anti-proliferative activity of EMILIN1.

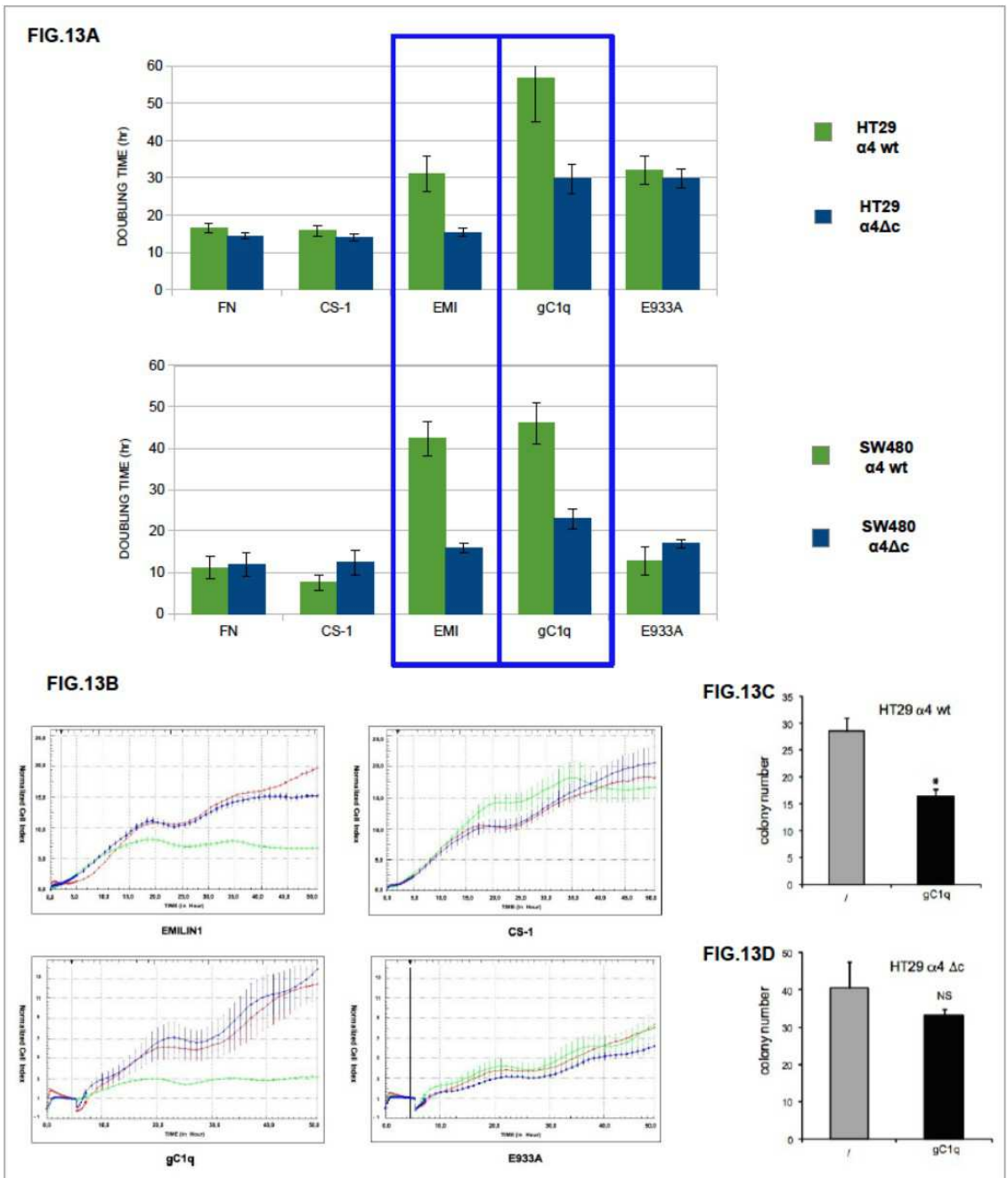

FIG.13) Cells growth is downmodulated by gC1q.
(A) Doubling time of HT29 and SW480 cells transfected with the wild type (wt) or the deleted α4 integrin chain and plated on Fibronectin or its domain CS1, EMILIN1 or its domain gC1q or E933A gC1q. (B) The same experiment but the normalized cell index of HT29 cells transfected is shown. (C) HT29 cells transfected with the wild type (wt) or (D) the deleted α4 integrin chain and plated in 0.4% agar in the presence or in the absence of gC1q.

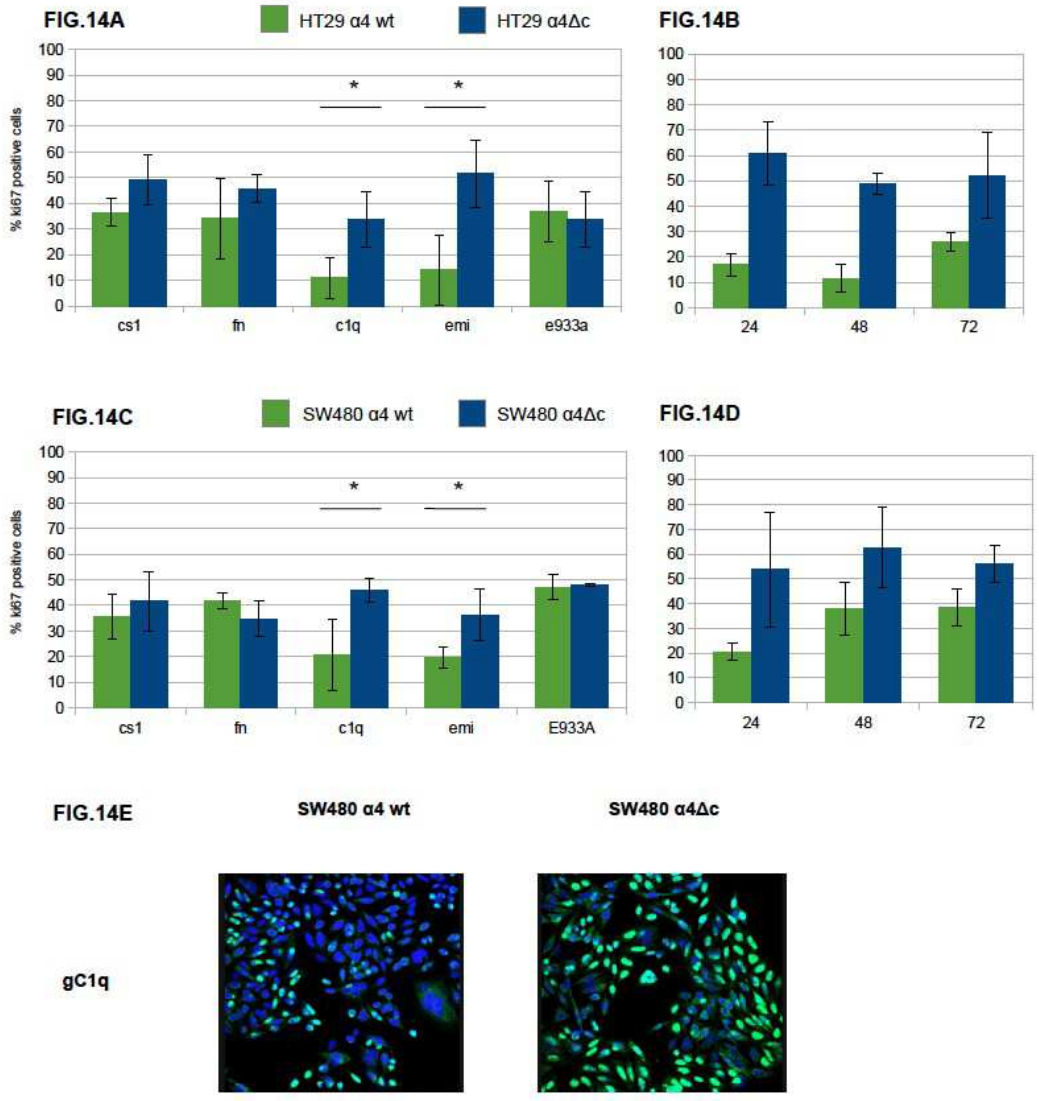

FIG.14) Ki67 immunofluorescence analysis:
A) HT29 and C) SW480 α4 WT transfected cells (green) grown on EMILIN1 and its domain gC1q show decreased levels of the proliferative marker Ki67 compared to α4Δc transfected cells (blue) on others ligands at 48h.
B) HT29 and D) SW480 α4 WT transfected cells (green) grown on gC1q show decreased levels of the proliferative marker Ki67 compared to α4Δc transfected cells (blue) at different time points.
E) Staining of the proliferative marker Ki67 for SW480 α4 WT and α4Δc transfected cells.

4.3) EMILIN1 SILENCES THE RAS-ERK PATHWAY VIA α4β1 INTEGRIN

4.3.1) Downstream effects of persistent cell adhesion to gC1q

To investigate the downstream signalling leading to reduced proliferation following α4β1-dependent cell adhesion to EMILIN1/gC1q, HaCat keratinocytes persistently adherent to gC1q were assayed (i.e. after 24h adhesion). Phosphorylation of FAK (Tyr925) generates a binding site for SH2 bearing molecules and triggers a RAS-dependent activation of the MAP kinase pathway (Schlaepfer *et al. 1*994). Only FAK (Tyr925) incremented if compared to polylysine attachment, whereas FAK (Tyr397) did not change (**FIGURE 15A**). On the contrary, pERK1/2 was dramatically reduced on gC1q at these late times of adhesion.

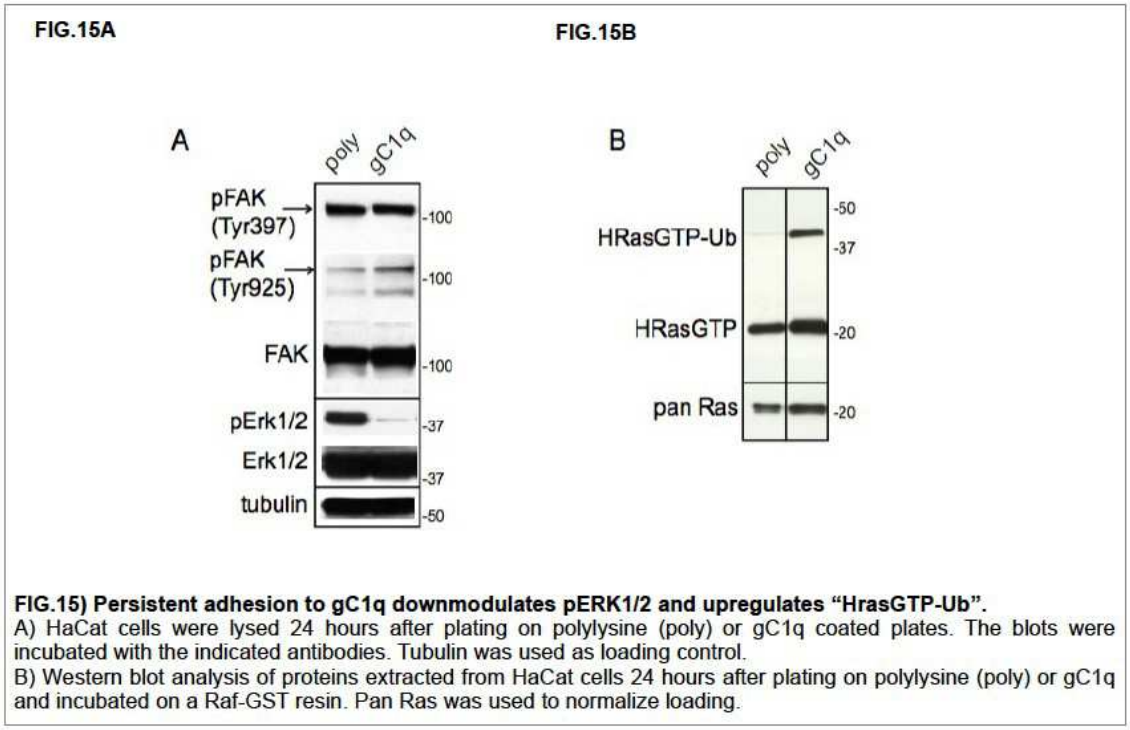

FIG.15) Persistent adhesion to gC1q downmodulates pERK1/2 and upregulates "HrasGTP-Ub".
A) HaCat cells were lysed 24 hours after plating on polylysine (poly) or gC1q coated plates. The blots were incubated with the indicated antibodies. Tubulin was used as loading control.
B) Western blot analysis of proteins extracted from HaCat cells 24 hours after plating on polylysine (poly) or gC1q and incubated on a Raf-GST resin. Pan Ras was used to normalize loading.

To test if the active form of HRas (HRasGTP) was involved in cellular signals triggered by EMILIN1/gC1q, a HRasGTP pull-down assay was performed on HaCat cells plated on gC1q or polylysine and analysed 24h after plating. HRasGTP increased in cells plated on gC1q compared to polylysine (**FIGURE 15B**).

In addition to the HRasGTP 21 kDa band, an upper band of about 40 kDa was detected by the anti HRas antibody (**FIGURE 15B**). Beside the canonical 21 kDa, RAS proteins display a plethora of faster and slower bands corresponding to the post-translational modified forms or to the mono- (30 kDa) and di-ubiquitinated (40 kDa) forms, respectively (18-21). In our experiments the intensity of the 40 kDa band,

corresponding to the di-ubiquitinated HRasGTP (HRasGTP-Ub) form, was several-fold higher on gC1q compared to polylysine, suggesting that, following α4β1 integrin activation as a consequence of cell adhesion to gC1q, HRasGTP could be ubiquitinated.

4.3.2) The HRas-ERK1/2 pathway is inactivated via the α4 integrin chain

To determine if the downstream consequences of cell adhesion to gC1q were dependent on a mechanism specifically due to the ligation of the α4β1 integrin, we compared the extent of di-ubiquitinated HRasGTP in cells adherent to gC1q to that detected in cells adherent to collagen type I that uses a different integrin as cellular receptor. As depicted in **FIGURE 16** both the anti ubiquitin antibody as well as the anti HRas antibody recognized proteins whose migration corresponded to the HRasGTP di-ubiquitinated form. HRasGTP-Ub was 10 times less in cells adherent to polylysine as well as to collagen type I compared to gC1q (**FIGURE 16**), suggesting that the α4 dependent signalling was qualitatively/quantitatively distinct and specific. Accordingly, while the ratio of HRasGTP-Ub/HRasGDP-Ub was about 0.5 in cells adherent to either polylysine or collagen type I, this ratio was 10-fold in cells adherent to gC1q, indicating that in α4 dependent cell adhesion there is a specific switch from RasGDP to RasGTP.

The results obtained so far strongly suggested that the α4β1 integrin dependent cell adhesion to gC1q was responsible for the subsequent ubiquitination of the activated HRas (HRasGTP) and this in turn down-regulated the extent of ERK1/2 phosphorylation, with an inverse correlation between the levels of these two molecules (**FIGURE 15**).

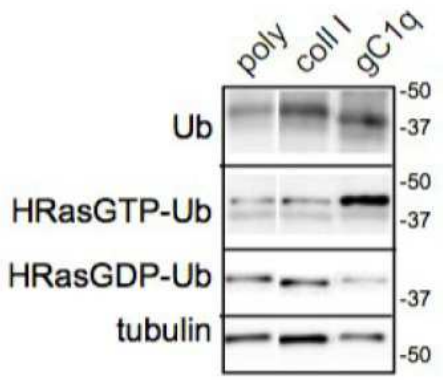

FIG.16) Only persistent adhesion to gC1q via α4β1 integrin upregulates the di-ubiquitinated HrasGTP. Western blot analysis of proteins extracted from HaCat cells 24 hours after plating on polylysine (poly), collagen type I or gC1q and incubated on a Raf-GST resin. Tubulin was used as loading control.

4.3.3) The gC1q ligated α4 integrin chain is physically linked to HRas

The cells were plated on polylysine, collagen type I, or gC1q for 24 hours and at the end of the incubation the cells lysates were immunoprecipitated with the α4 antibody, separated on a reduced 4-20% gel, and immunoblotted with anti HRas antibody. As expected the α4 integrin chain was immunoprecipitated from cells adherent on every ligand; however, the ubiquitinated form of HRas (40 kDa mass) co-immunoprecipitated with the α4 integrin chain only in cells plated on gC1q (**FIGURE 17**). In fact, a band at the expected molecular mass was detected in the lysate and in the unbound cell lysate when probed with anti HRas antibody. Here, the HRasGTP and HRasGDP ubiquitinated forms cannot be distinguished since the lysates were co-immunoprecipitated and not pulled down for HRasGTP. However, as shown in **FIGURE 16**, it is very likely that the co-immunoprecipitated HRas-Ub, in cells plated on gC1q, is primarily due to the HRasGTP membrane-bound form.

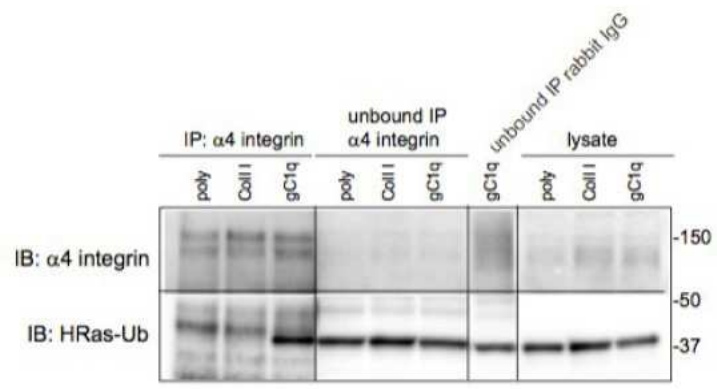

FIG.17) HRas-Ub is co-immunoprecipitated with the α4 integrin chain. HaCat cells were lysed 24 hours after plating on polylysine (poly), collagen type I (Coll I) or gC1q coated plates. Lysates were immunoprecipitated with the α4 antibody and immunoblotted with anti α4 antibody and anti HRas antibody.

To further examine the possible link between α4β1 dependent cell adhesion, RAS and ERK1/2 activation, and cell proliferation, stably transfected HT29 cells were let adhere to gC1q or collagen type I for 24h. Immunoblotting of cell extracts indicated the following: the ratio of HRasGTP-Ub/HRasGDP-Ub in cells transfected with the wild type α4 WT integrin chain and adherent on collagen type I was around 1.0; on the contrary and in analogy with data obtained on HaCat cells (**FIGURE 16**), this ratio was around 4.0 in cells adherent on gC1q (**FIGURE 18**). The likely explanation is that after its activation HRas-GTP was directed towards ubiquitination. To confirm that this pathway depended on the presence of a fully functional α4 integrin chain we examined

cells transfected with the deleted α4 integrin chain. In this case the ratio of HRasGTP-Ub/HRasGDP-Ub in cells adherent on gC1q decreased accordingly compared to cells transfected with the wild type α4 integrin chain (**FIGURE 18**).

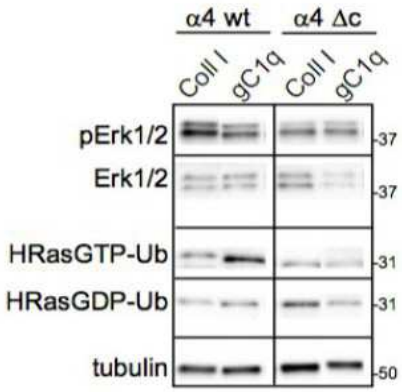

FIG.18) Modulation of HRas-Ub and pERK1/2 in α4 integrin chain transfected HT29 cells. HT29 cells were lysed 24 hours after plating on collagene type I (Coll I) or gC1q coated plates. The blots were incubated with the indicated antibodies. Tubulin was used as loading control. Cell lysates were pulled down on a Raf-GST resin to isolate HrasGTP-Ub.

To summarize, I confirmed the fundamental role of the residue E933A and of the cytoplasmic tail of the α4 integrin and how they are involved in an anti-proliferative function. Finally, I demonstrated that the interaction between α4 and EMILIN1 deactivates the MAPK pathway through HRas (**FIGURA 19**) and this pathway depend on the presence of a fully functional α4 integrin chain.

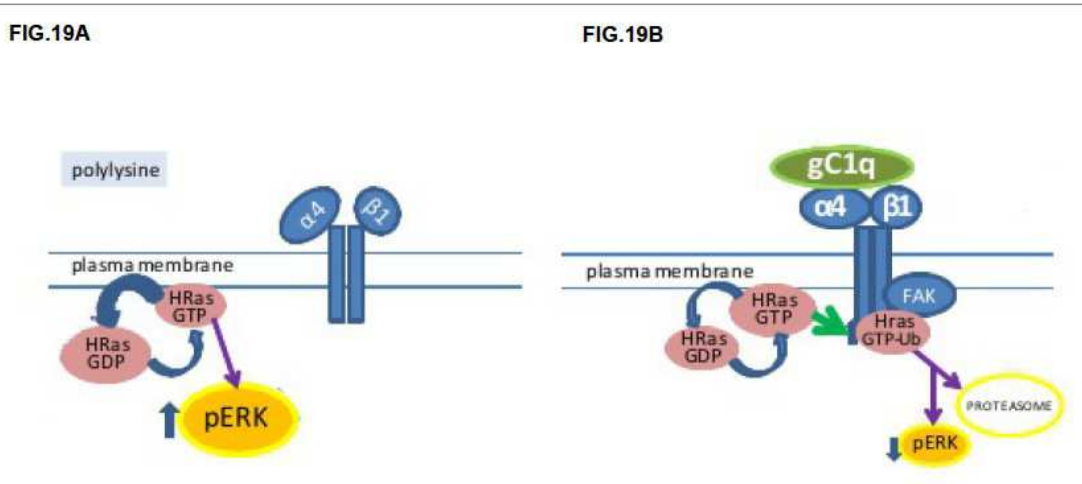

FIG.19) A schematic view of the HRas involvement in gC1q α4 integrin mediated pathway. (A) In cells plate on polylysine the α4β1 inactive integrin is not able to induce HRas activation. (B) Activation of α4β1 integrin, mediated by gC1q, through FAK induces HRasGTP increase as well as its ubiquitination (HRasGTP-Ub). HRasGTP switching off (along with low basal level of intracellular Ca2+) is able to reduce ERK1/2 phosphorylation and proliferation.

4.4) α4β1 AND EMILIN1 EXPRESSION HUMAN COLON

First, I demonstrated that α4 is expressed on intestinal epithelial cells (IEC) but it is absent in several colon cancer cell lines (**FIGURE 8**). Then, I checked the expression of α4 in human colon tissues and found that compared to normal tissues, in human tumor colon samples there was a strong down-regulation of its expression (**FIGURE 20A**). But what about EMILIN1? Even in this case I compared normal and tumor colon human tissues and I observed a down-regulation in human tumor colon samples for EMILIN1 (**FIGURE 20B**).

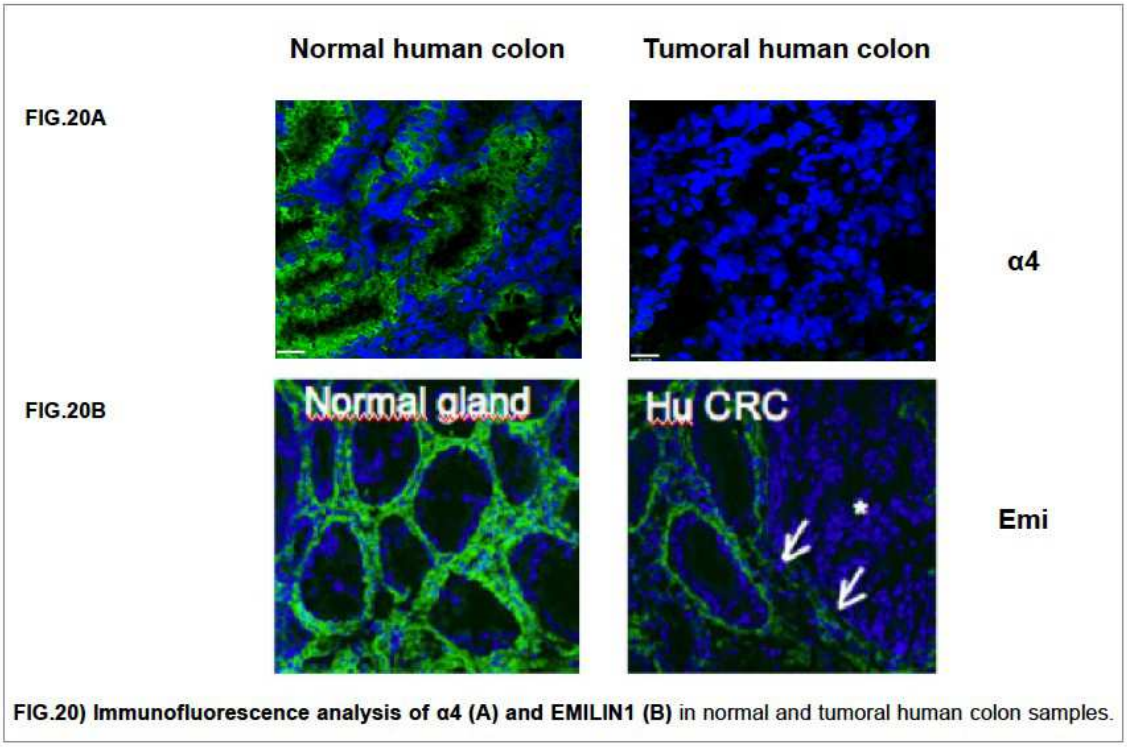

FIG.20) Immunofluorescence analysis of α4 (A) and EMILIN1 (B) in normal and tumoral human colon samples.

4.5) THE E933A TRANSGENIC MOUSE MODEL

In previous studies it was demonstrated that EMILIN1 plays a role in the homeostatic control of cell proliferation in the skin (Danussi *et al.* 2011) and a protective effect in a two-stage model of DMBA induced skin carcinogenesis (Danussi *et al.* 2012). To further investigate the putative function of EMILIN1 in a different cellular setting, we first determined that also colon crypts of FVB/N EMILIN1 KO mice compared to WT littermates are larger and have more Ki67 positive cells suggesting that an EMILIN1 deprived microenvironment might promote higher tumor development also in colon.

Emilin1 null mice have increased TGF-β levels (Zacchigna *et al.* 2006; Danussi *et al.* 2011) because of the lack of regulation on the pro-TGF-β processing. To verify the role of EMILIN1 and in particular of the single E993 residue in the complex scenario of colitis (inflammation) and colon cancer (inflammation associated colon cancer) a E933/EMILIN1 transgenic mice (TG) was generated that could display normal TGF- β levels while having highly reduced or no possibility to show cell adhesive capability for α4β1. Very briefly, three independent mouse transgenic lines were generated and in one of these the expression of the human *Emilin1* gene was equivalent to that of the endogenous murine gene (**FIGURE 21**). Mice were then crossed to EMILIN1 KO mice in order to avoid the expression of the mouse EMILIN1 protein and have only the expression of the mutated human E933A protein.

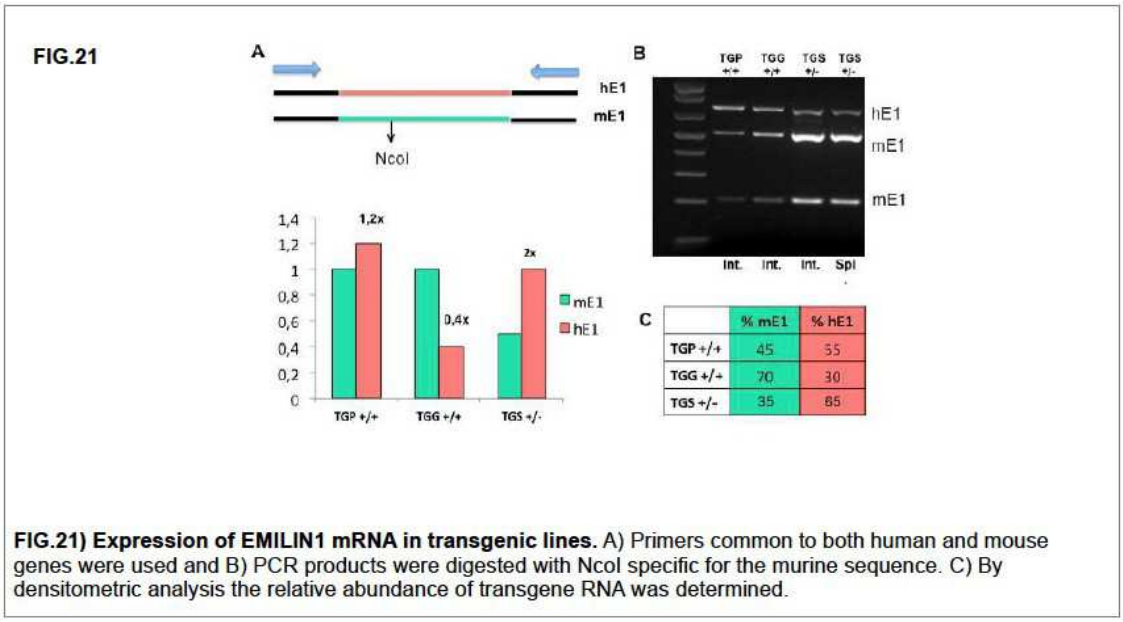

FIG.21) Expression of EMILIN1 mRNA in transgenic lines. A) Primers common to both human and mouse genes were used and B) PCR products were digested with NcoI specific for the murine sequence. C) By densitometric analysis the relative abundance of transgene RNA was determined.

Several tissues of the E933A strain were checked for EMILIN1 expression by immunofluorescence and the colon expressed the human transgenic protein at good levels compared to the WT (**FIGURE 22**).

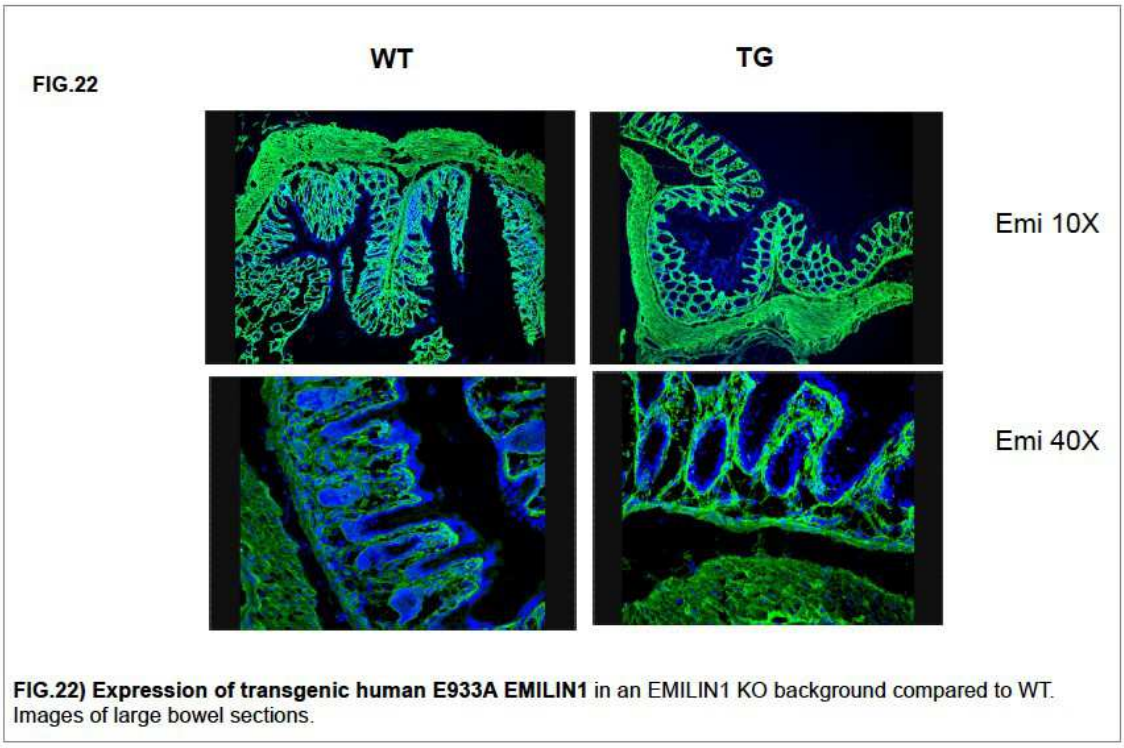

FIG.22) Expression of transgenic human E933A EMILIN1 in an EMILIN1 KO background compared to WT. Images of large bowel sections.

4.5.1) EMILIN1 E933A transgenic mice present an hyperproliferative phenotype in the colon

A comparative analysis between WT and TG colon specimens was performed. Histological analysis of the colon of TG mice showed an increased epithelial thickness (at day 30) compared with WT mice (**FIGURE 23A**). No differences were observed in the number of active caspase-3–positive cells in the colon of WT and TG mice (not shown); the thickness of mutant mice was associated with a marked increase in Ki-67 immunoreactive nuclei (**FIGURE 23B e 23C**). TG colon crypts displayed a significant increase in the proliferation rate compared with WT suggesting that an EMILIN1 E933A microenvironment promotes an higher proliferative compartment in accord with the skin model.

4.5.2) EMILIN1 WT and E933A newborn isolated mouse fibroblasts show altered proliferation

Fibroblasts were isolated from the skin of newborn WT and transgenic E933A mice and cultured for at least two weeks, then were grown on cover-glass slides for 48 hours and were stained with the proliferation marker Ki-67 and α4 expression was analyzed by FACS (**FIGURE 24A**).

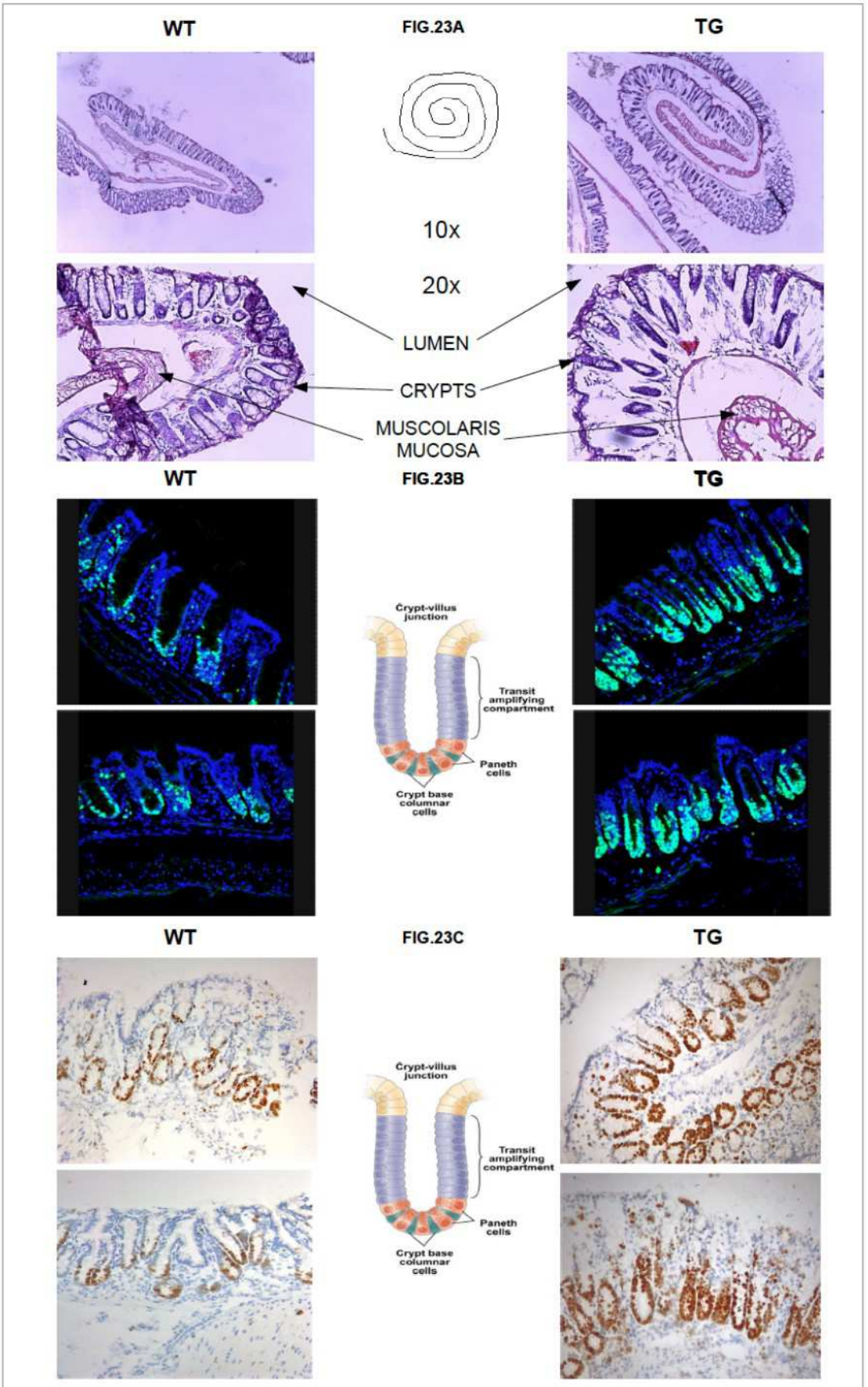

FIG.23) Colon hyperplastic phenotype in *Emilin1 TG* mice. A) Hematoxylin and eosin (H&E)-stained colon cryostat Swiss Roll sections from WT mouse (left) and TG mouse (right). Colon crypts of EMILIN1 TG mice show higher proliferation as detected by immunofluorescence (B) and immunochemistry (C) Ki67 staining.

A higher proliferation rate in newborn fibroblasts isolated from E933A mice skin compared to the fibroblasts isolated from WT mice was measured (**FIGURE 24 B and C**). In this scenario, the expression of E933A mutated human EMILIN1 provides an *ex vivo* proof of the anti-proliferative role of EMILIN1. The role of the interaction with α4 integrin is important for the anti-proliferative effect in fibroblasts.

FIG.24A

	ABCAM	PS-2
WT **NBIMF**	77%	53%
TG **NBIMF**	75%	60%

FIG.24B

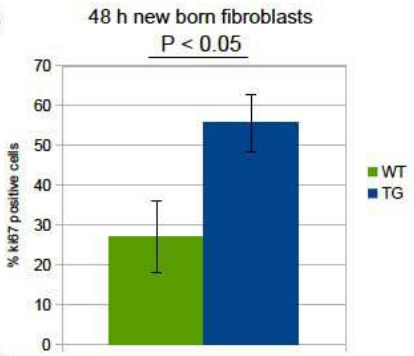

FIG.24C

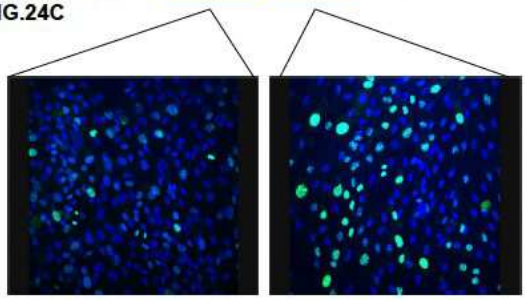

FIG.24) EMILIN1 WT (green) and E933A (blue) new born isolated mouse fibroblasts (NBIMF 3°pass) show same α4 expression measured both with a PS-2 Ab from ABCAM and a PS-2 home made (A) E933A NBIMF had an increased % of Ki67 positive cells (B) as shown from immuofluorescence staining (C).

4.6) DSS-INDUCED EXPERIMENTAL COLITIS

Considering the particularly prominent role of α4β1 in the immune system, I investigated its involvement in colitis. To determine if the TG background influences the extent of inflammation, WT and TG mice were acutely or chronically treated with DSS 3% in the drinking water and clinical (DAI index) and endoscopic (MEICS index) parameters compared.

In both acute and chronic inflammation DAI index was worse in TG than in WT mice (**FIGURE 25D and E**): TG mice lost more weight and presented more rectal bleeding and diarrhea. In addition, the level of colonic tissue destruction observed was dramatically increased among TG mice, when examined at the termination of the acute treatment (on day 7), as measured by the colon length (**FIGURE 25B**).

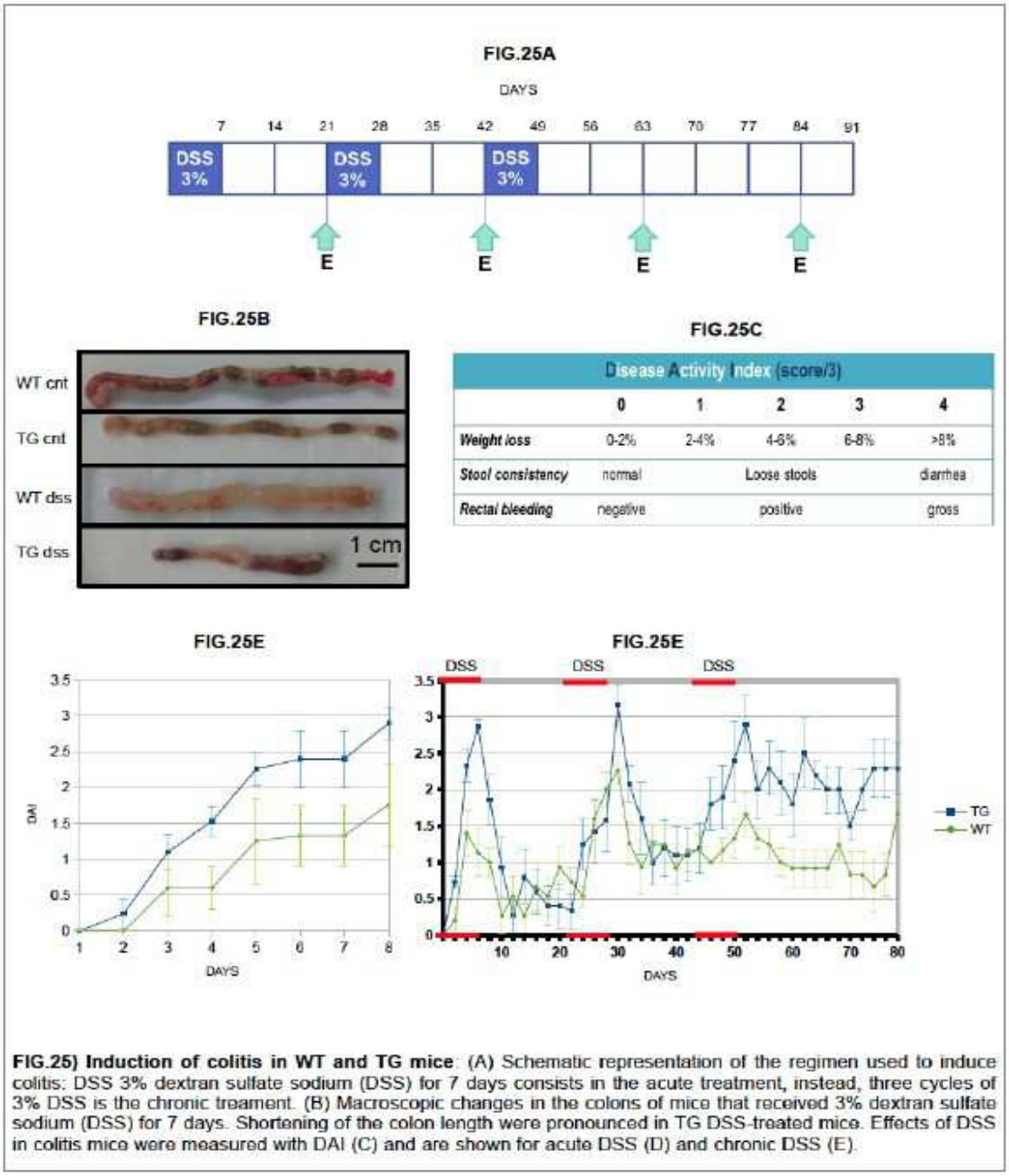

FIG.25) Induction of colitis in WT and TG mice: (A) Schematic representation of the regimen used to induce colitis: DSS 3% dextran sulfate sodium (DSS) for 7 days consists in the acute treatment, instead, three cycles of 3% DSS is the chronic treament. (B) Macroscopic changes in the colons of mice that received 3% dextran sulfate sodium (DSS) for 7 days. Shortening of the colon length were pronounced in TG DSS-treated mice. Effects of DSS in colitis mice were measured with DAI (C) and are shown for acute DSS (D) and chronic DSS (E).

To confirm the colitis disease I performed endoscopy in both treatments. Whereas Wild-Type mice showed only mild alterations of the mucosal surface with a moderate murine endoscopic index of colitis severity (MEICS), TG mice displayed signs of severe colitis with higher MEICS score (**FIGURE 26A**). Accordingly, the endoscopy of TG mice showed a thickening of the bowel wall, alterations of the vascular pattern, and a more granular mucosa with high amounts of fibrin in the lumen (**FIGURE 26B**).

FIG.26A

Murine Endoscopic Index of Colitis Severity				
	0	1	2	3
Thickening of the colon	transparent	moderate	marked	Non transparent
Changes in the vascular pattern	normal	moderate	marked	bleeding
Fibrin visible	none	little	marked	extreme
Granularity of the mucosal surface	none	moderate	marked	extreme
Stool consistency	Solid/normal	Still shaped	unshaped	spread

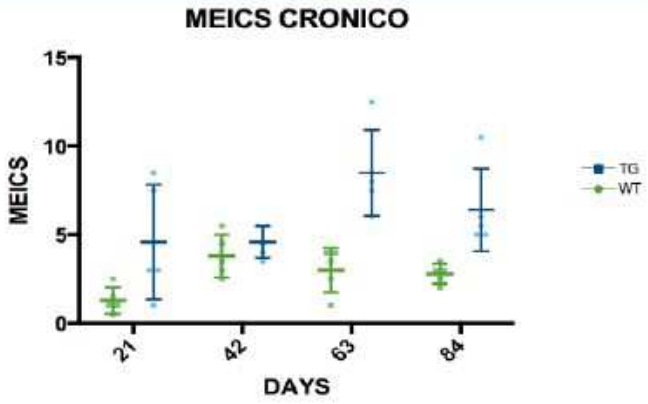

FIG.26B

FIG.26) Murine endoscopic index of colitis severity (MEICS): the five parameters of the murine endoscopic index of colitis severity (MEICS) were determined (A). Representative endoscopy images indicating severe colitis in TG mice (B).

The histopathological analysis are in line with the endoscopic findings of colon samples. DSS chronically treated WT mice showed only low histologic scores, in contrast, TG mice demonstrated scores indicative of severe colitis, as shown by epithelial erosions (damage of the superficial epithelium), presence of small lymphoid follicles and and massive infiltrations into the mucosa (numerous inflammatory cells between the glandular structures) (**FIGURE 27A**). The increased pathology observed, in chronically treated TG mice, occurred in association with increased levels of

myeloperoxidase (MPO) and lymphocytes (CD3) in TG colon tissue (**FIGURE 27B and 27C**) and finally even with an increased of small follicles number.

All these data are summarized in **FIGURE 27D**. The **FIGURE 27D** give us also the Ki-67 % of mucosa and of gland: in the control mice, there were a marked increase in Ki-67 immunoreactive positive cells in the lower part of the crypt as shown in **FIGURE 23C**. The anti-Ki-67 positive cells were reduced in the mice fed with DSS but the difference between the WT and TG mice remain (**FIGURE 28**).

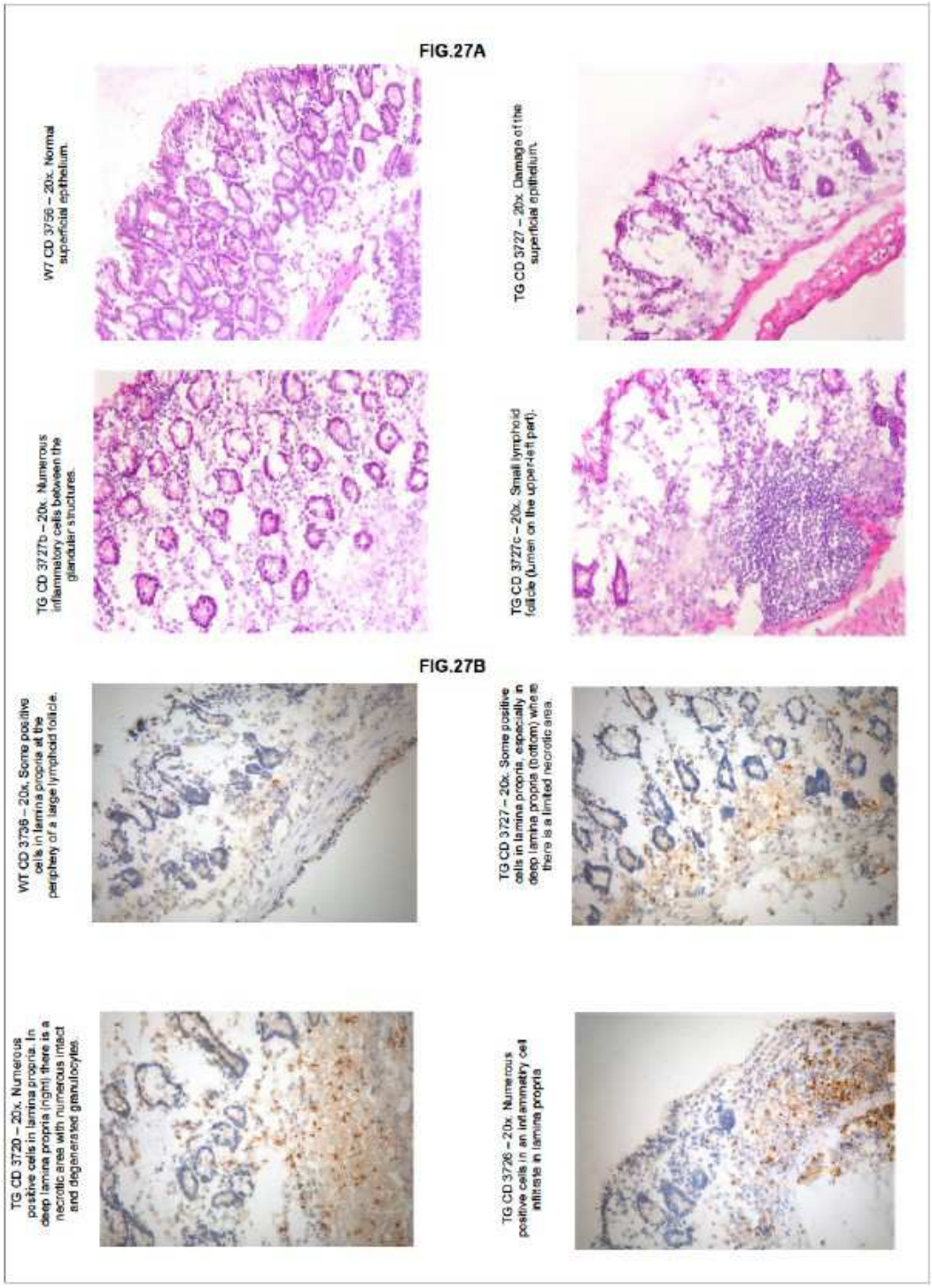

FIG.27C

WT

TG

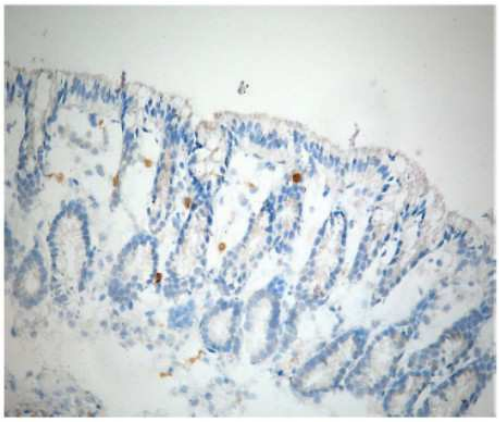

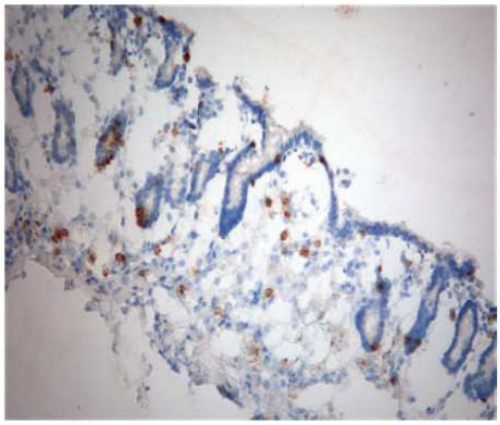

WT CD 3756 – 20x. Few T lymphocytes in lamina propria.

TG CD 3627 – 20x. Numerous T lymphocytes in lamina propria and some intraepithelial.

FIG.27D

	histopathology				immunohistochemistry				
	epithelial damage	LP infiltrate	small follicles	large follicles	CD3	CD45/ B220	MPO	Ki67 % of mucosa	Ki67 % of gland
TG Acute DSS	1.2	1.6	0.4	0.8	3.6	1.4	2.6	**48**	50
WT Acute DSS	2.6	1.8	0.4	0.2	3.8	1.8	2.8	**26**	34
TG Acute CNT	0	0	1.3	0.3	2.6	1	0	**100**	46.6
WT Acute CNT	0	0.3	0	0	2.6	1	0.6	**93.3**	43.3
TG Chronic DSS	**0.4**	**1.6**	**2.8**	1	**3.4**	1	**2.6**	**72**	42
WT Chronic DSS	**0**	**0.75**	**0.75**	1.5	**2**	1	**1.5**	**55**	47.5
TG Chronic CNT	0	0	1	0	2.6	0.6	1	**90**	46.6
WT Chronic CNT	0	1	1	0.5	2.5	1	1.5	**85**	45

FIG. 26) Histopathological changes in colon tissue after chronic DSS treatment. Sections were stained with hematoxylin and eosin (H&E) and then examined with a light microscope for the detection and quantification of histological lesions (A). Sections immunostained with MPO (B) and CD3 (C). Summary of results are reported in FIG (D).

These results suggest what other studies demonstrated, that DSS induced cell cycle arrest, especially at the G0 phase. Ki-67 immunohistochemistry showed that cells with cell cycle arrest at the G0 stage in the crypt increased approximately "2-fold" as compared to the controls (**FIGURE 27D**).

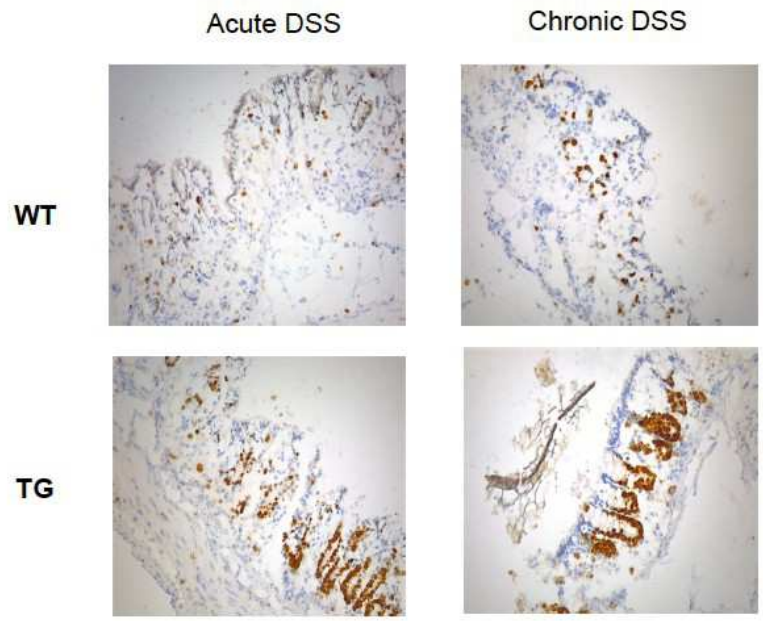

FIG. 28) Immunochemistry Ki67 staining of acute treatment (left) and chronic samples (right).

EMILIN1 is expressed both in normal and colitis tissues but it can be appreciated that there is a different expression of the α4 integrin between these two conditions: in the unaffected tissue the integrin is present only in the epithelial layer; on the other hand, in the inflamed tissue there is a diffuse distribution also outside the epithelial layers, suggesting that α4 is expressed on leucocytes (CD45-positive?) cells and much less on epithelium (**FIGURE 29**).

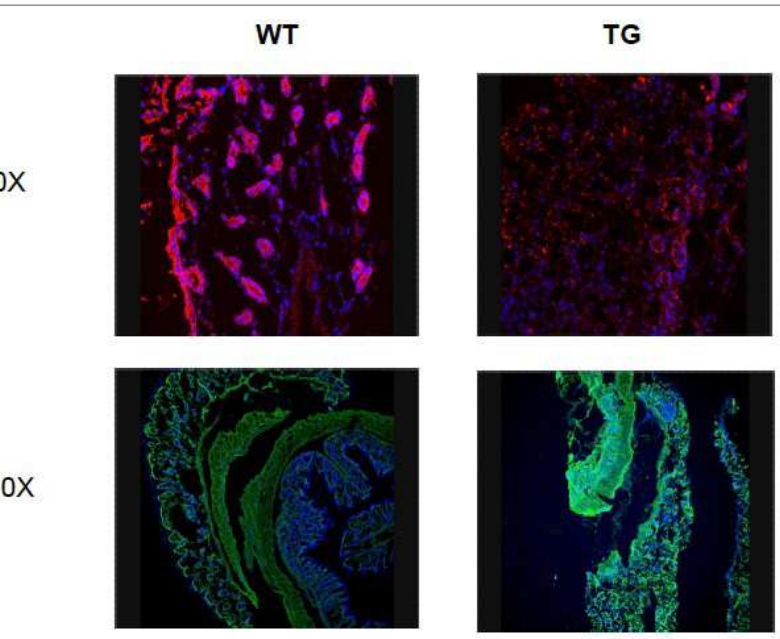

FIG. 29) α4 and EMILIN1 immunofluorescence staining of chronic samples.

Even if the expression of α4 and its presence on inflammatory cells remains to be formally proven, it is suggestive that the interaction of α4β1 with EMILIN1 might play an important role during colitis.

4.7) TWO STEP-COLON CARCINOGENESIS (AOM-DSS)

Given the antiproliferative results *in vitro* and the higher inflammation of TG DSS treated mice I hypothesized that the lack of the interaction between α4 and EMILIN1 could be involved also in tumor development. Colon tumors were induced with a single intraperitoneal injection of azoxymethane (AOM) followed by 1-week exposures to 3% Dextran Sodium Sulfate (DSS) in the drinking water. The AOM-DSS-treated mice develop tumors in the colon, the site of tumor formation in humans with mutated APC: in fact, this mouse model recollects the human tumor situation with persistent cycles of tissue damage and repair. Inflammation and tumor growth were observed over time by colonoscopy and clinical scoring of colitis severity was performed applying the MEICS endoscopic index.

However, in contrast to our initial hypothesis and quite surprisingly I obtain that TG mice had lower incidence, less and smaller tumors and better survival (**FIGURE 30**).

In line with this observations, when I examine/investigate the inflammation, MEICS values were worse in WT than in TG mice except in the early phases of the stimulations (day 21) (**FIGURE 31**).

In conclusion, even if the TG mice loose more weight and present more severe inflammatory parameters in the DSS induced colitis although they paradoxically develop less and smaller tumors in the two steps-colon carcinogenesis experiments.

Furthermore, TG mice present an hyperproliferative phenotype, nevertheless, our analysis revealed that TG tumors were smaller.

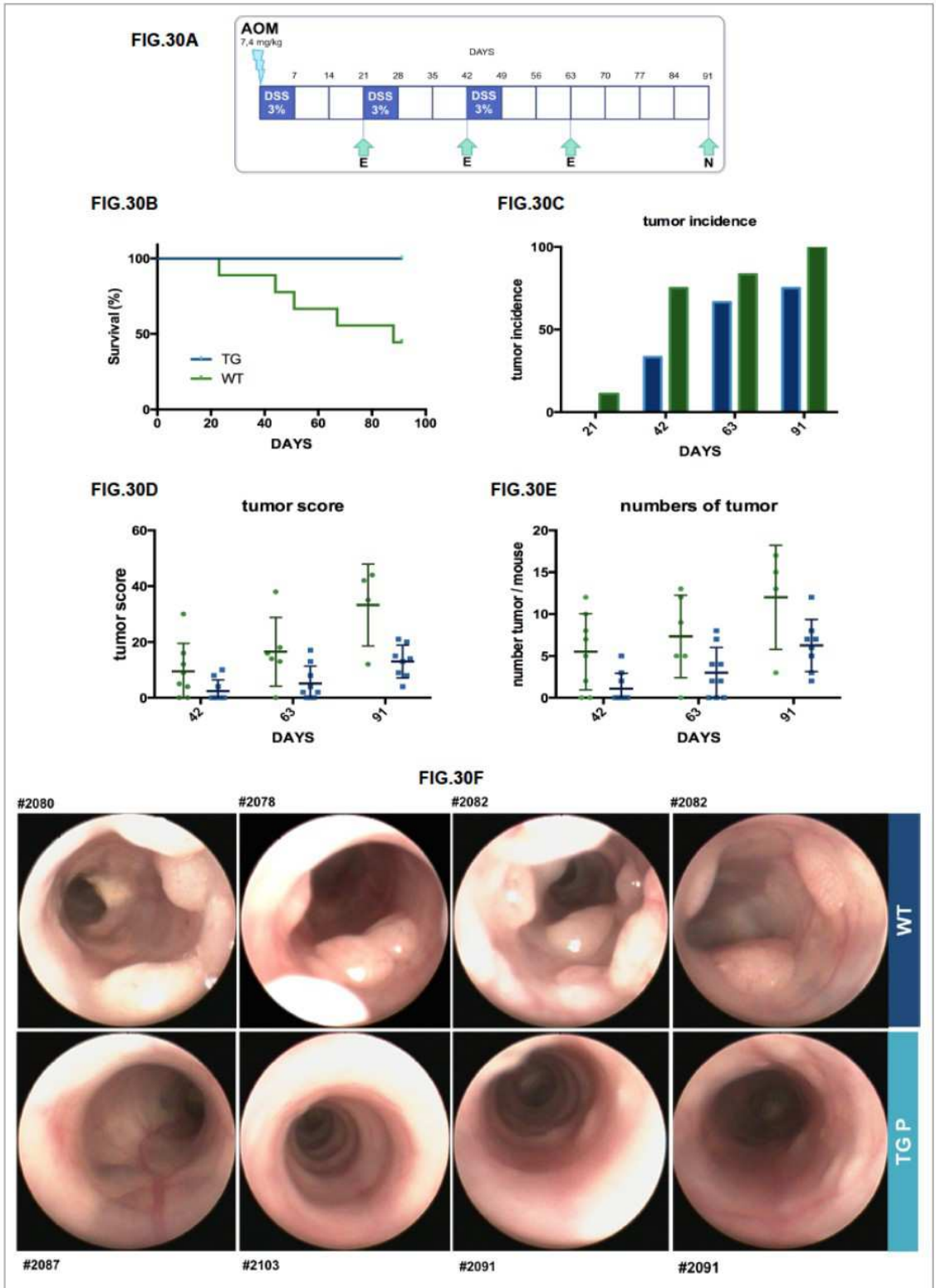

FIG. 30) E933A TG mice are less susceptible to colitis-associated cancer (CAC). (A) Schematic representation of the regimen used to induce CAC, whereby a single AOM injection (10 mg/kg body weight) is followed by three cycles of 3% DSS provided ad libitum in the drinking water. Tumour development was monitored by endoscopy at the indicated times (days) post-AOM treatment (denoted by 'E' in the schematic). B) Mortality rate of the mice with CAC. The survival of the mice was scored daily and is presented as a percentage; 100% denotes the survival (%) of the mice at the beginning of the experiment; Endoscopy tumour score indicates that WT mice exhibit increased incidence of CAC (C); tumour number (D) and total tumour (E) per mouse are elevated in WT mice compared to TG mice. (F) Representative endoscopy images indicating the presence of tumours in the distal portion (final 2.5 cm) of the colon at day 63 post-AOM injection.

Murine Endoscopic Index of Colitis Severity				
	0	1	2	3
Thickening of the colon	transparent	moderate	marked	Non transparent
Changes in the vascular pattern	normal	moderate	marked	bleeding
Fibrin visible	none	little	marked	extreme
Granularity of the mucosal surface	none	moderate	marked	extreme
Stool consistency	Solid/normal	Still shaped	unshaped	spread

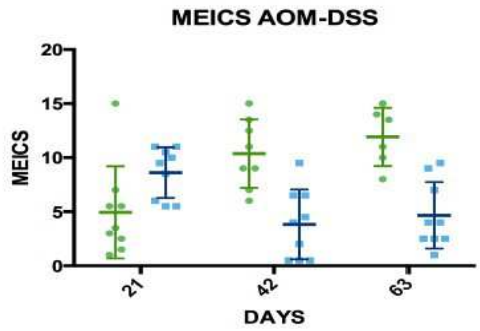

FIG. 31) MEICS of AOM-DSS treatment.

4.8) MURINE COLON LEUKOCYTE GLOBAL IMMUNE PHENOYPE ANALYSIS

To investigate the paradox of a higher inflammation rate in E933A mice but a reduced tumor burden I achieve a murine colon leukocytes isolation to perform a global immune phenotype analysis. The goal here was to understand the quality of inflammation instead of the quantity: the analysis of the cells focus on the composition of the subpopulations. This gives an opportunity to compare various situations of the mucosa in different groups. The cells are stained with antibodies for CD4+, CD8+, CD11b+ and CD11c+ to cover main cell populations. First, I investigated the several subpopulations in the blood samples taken from the acute DSS treated mice (**FIGURE 32B**). In the TG mice I found a general decrease of CD45+ cells and worthy of attention an increased number of CD8+ cells and a decrease number of CD4+ cells. Very interesting the level the ratio CD8/CD4 was increased also in samples originated from the epithelial layer of the colon of TG mice DSS acutely treated where I found also an increase of CD3+ cells (**FIGURE 32C**) in line with immunochemistry analysis (**FIGURE 27C**). Increased numbers of CD8+ T cells (and less CD4+ T cells) can be observed also from the colon originated from TG mice DSS chronically treated (**FIGURE 32D**).

Finally, the resulting numbers of CD8 and CD4 is different in TG compared to WT (**FIGURE 32E**) and changes in this type of subpopulation could explain the decrease of tumor burden in TG mice.

FIG.32A

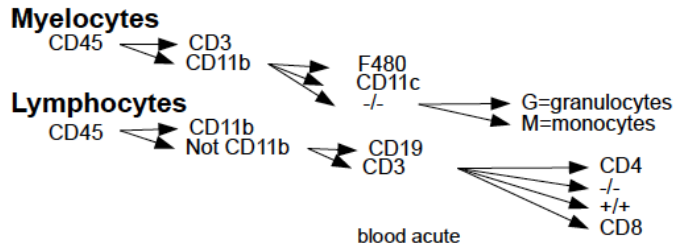

FIG.32B

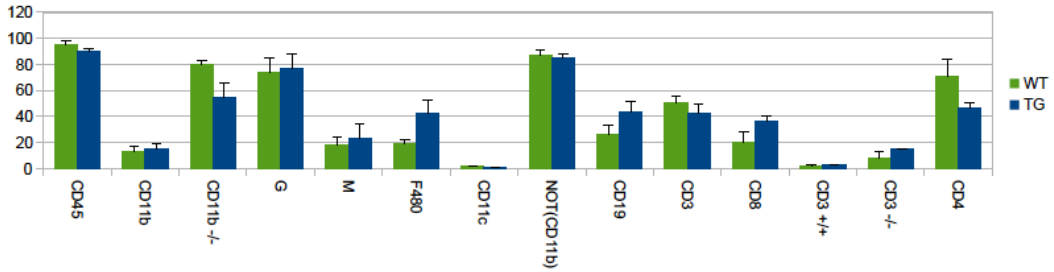

FIG.32C

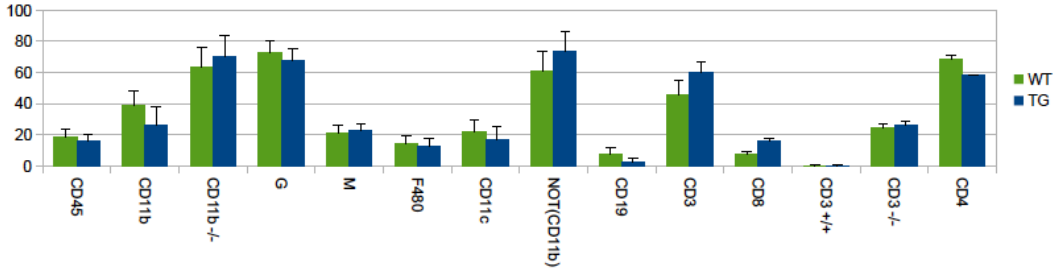

FIG.32D

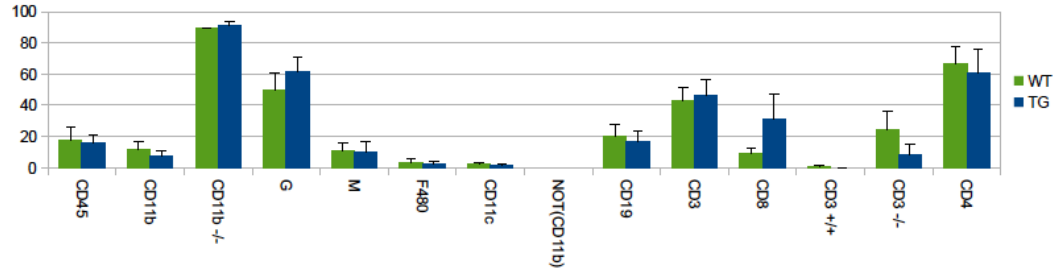

FIG.32E

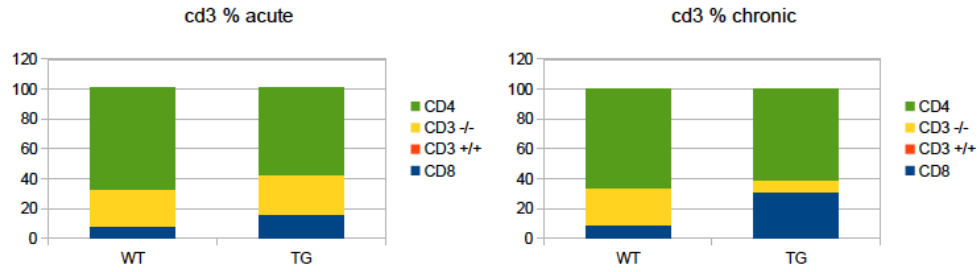

FIG. 32) Leukocytes global immune phenotype analysis: (A) Setting of hierarchy myelocytes and lymphocytes subpopolations; analysis of blood samples after acute treatment (B); analysis of colon sample, in particular the epithelial layer, after acute (C) and chronic (D) treatment with the % of CD3 subpopulations (E).

5) DISCUSSION

EMILIN1 mediates α4β1-dependent cell adhesion through its globular trimeric gC1q domain (Spessotto *et al.* 2003). The accurate and elegant three-dimensional model of the isolated recombinant EMILIN1 gC1q trimer, produced and purified in our laboratories, was determined by NMR spectroscopy studies (Verdone *et al* 2008 and 2009) and provided evidences that constituted the structural basis for my functional analyses.

The quaternary structure of EMILIN1 gC1q assembly identified, for each monomer, a unique unstructured loop (spanning from Y927 to G945 residue) located at the apex of the homotrimer and available for interactions with ligands/receptors. The attention was focused on E933 residue occurring in the unstructured segment Y927–G945: the E933A mutation fully inhibited Jurkat T cell adhesion (Spessotto *et al.* 2003). E933 appears to play an absolutely central role in α4β1-integrin mediated interaction with the EMILIN1 gC1q domain, whereas several residues close to E933 do not seem to participate in the major interaction sites between the two molecules. The NMR structure locates residue E933 in a flexible loop structure at the apex of the EMILIN1 gC1q domain assembled into a symmetric trimer; once the stoichiometry of three integrin molecules for a single gC1q trimer is ruled out for steric reasons, the interaction pattern with α4β1 might well entail binding of three E933 to the integrin ligand-binding region or the need of just one E933 residue for a proper interaction with the integrin ligand. One possibility to tackle this question is the use of bicistronic vectors coding for wild type and non-functional mutant E933A gC1q in order to obtain trimers with a single copy or two copies of the wild type (WT) sequence in the homotrimer. In this system the mutant and WT monomers are randomly assembled into trimers to form a heterogeneous population and can be isolated by affinity chromatography. Preliminary data suggests that cell adhesion to heterogeneous gC1q trimers, composed by both wild type and E933A mutants, is negatively affected implying the need of all three wild type monomers to achieve a proper integrin ligation with the homotrimer (Capuano *et al.* in preparation).

The major aim of the present study was to analyze in detail the mechanisms and the putative functional repercussions of the interaction between the ECM protein EMILIN1 and the integrin cell receptor α4β1. First fibroblastic cells expressing α4β1 deposit WT EMILIN1 in the ECM; on the contrary, E933A EMILIN1 transfectants show a marked decrease in EMILIN1 staining, suggesting alterations in extracellular deposition. These

results are consistent with the hypothesis that the E933A mutant exerts a dominant negative effect on the endogenous EMILIN1-integrin interaction (Capuano *et al.* in preparation) and thus affects the regular EMILIN1 network organization in the ECM. This autocrine system was useful to confirm that the E933 residue of EMILIN1 is fundamental for the adhesion of gC1q and its binding with α4 is of great importance to allow an anti-proliferative activity. In fact, when EMILIN1 interacts with cells expressing the α4β1 integrin there is a significant down-regulation of cell proliferation. This reduced proliferation was reported also in a skin model (Danussi *et al.* 2011). All this data led me to hypothesize that the EMILIN1/α4 interaction could be potentially involved in a lower proliferation rates of colon epithelial cells and also in the regulation of colitis and colon carcinogenesis.

Accordingly, the paracrine system with colon epithelial cells transfected with α4β1 and in which EMILIN1 is provided as a recombinant protein substrate, to allow their interaction, show a significant down-regulation of cell proliferation. In addition, using *ITGA4* mutant sequences, I conclude that the cytoplasmic tail of α4 is responsible for the anti-proliferative function when it interacts with EMILIN1 or its globular gC1q domain.

This latter model was used also to study the signalling behind the anti-proliferative capability: the α4 chain, and not the truncated integrin α4 chain, promotes HRasGTP ubiquitination and affects ERK1/2 phosphorylation. This is provided by an integrin-dependent down-regulation of HRas signalling: integrin engagement by the gC1q triggers a series of events leading to the ubiquitination and likely degradation of HrasGTP. In turn, the loss of HrasGTP is responsible for pERK1/2 down-regulation and low proliferation linking the anti-proliferative capability of α4β1 to a proto-oncogene like HRas through the switching off of its activated form.

The EMILIN1/α4β1/HRas/pERK1/2 pathway is specific for the α4β1/EMILIN1 pair since cells persistently adherent to collagen type I via the α2β1 integrin do not show enhanced HRasGTP degradation and consequently, the levels of pERK1/2 are unchanged and the cell proliferation is not down-regulated. Moreover, the finding that the α4 integrin chain is co-immunoprecipitated with HRas-Ub only in cells adherent to gC1q and not to polylysine nor collagen type I confirms that there is a physical association between the α4 integrin chain and Hras-Ub (Modica *et al.* 2017).

Contrary to common beliefs that consider α4β1 an exclusive leukocyte integrin, there are some data available that demonstrates its expression in colon tissue and its

methylation in colitis and colon adenomas/carcinomas (Zhang *et al.* 2009; Ausch *et al.* 2009; Gerecke *et al.* 2015). I also found that *ITGA4* is not expressed on colon cancer cell lines but it is expressed on intestinal epithelial cells. Furthermore, α4 and EMILIN1 are deregulated in some human colon biopsy.

To clarify the involvement and the putative functional consequences of the interaction between EMILIN1 and α4β1 in the regulation of colitis and colon carcinogenesis I took advantage of an E933A transgenic mouse line (TG) available in the laboratory. These TG mice in which EMILIN1 is normally expressed but it does not interact with the α4β1 integrin have a more proliferative intestinal epithelial barrier presenting an hyperproliferative phenotype of the mucosa with increased epithelial thickness, increased Ki-67 in colon crypts and elongation of the proliferative compartment. In addition, EMILIN1 WT and E933A newborn isolated mouse fibroblasts show altered proliferation with TG cells displaying an increased proliferation compared to WT cells.

Using this TG model I found that EMILIN1 has a dual function in inflammation and in colitis-associated colorectal tumorigenesis. On one side, during DSS-induced experimental colitis, (at early stages of colon cancer), EMILIN1/α4 pair protects intestinal epithelial cells against proliferation (by regulating intestinal epithelial barrier function). Accordingly, EMILIN1 E933A TG mice display enhanced colitis-induced epithelial damage and inflammation. This is in line with the hyperproliferative phenotype of TG mice *in vivo* and with the inhibition of proliferation given by α4 transfected cancer colon cells *in vitro*. The inflammation was mirrored with a clinical index (DAI) and also with a colonoscopy score (MEICS): both scores confirm a worse and increased inflammation in TG mice than in WT. More specifically, during the chronic treatment there is higher accumulation of inflammatory cells with increased levels of myeloperoxidase (MPO) and more lymphocytes (CD3 positive cells) in TG colon tissue and also an increased number of small follicles. All the data collected indicate an enhanced proliferation in the TG mouse and the difference in proliferation between TG and WT mice are even higher compared to the basal level values during the DSS-induced experimental colitis.

Quite surprisingly, in the two-step colon carcinogenesis (AOM-DSS), TG mice display a reduction of tumor burden: lower incidence, less and smaller tumors and better survival.

Worthy of attention, colitis score values were worse in WT than in TG mice except in the early phases of the stimulations (day 21). Thus, EMILIN1 suppresses inflammation-

associated epithelial damage and proliferation but, at later stages, contributes to the tumorigenesis of tumor cells. EMILIN1/α4 had a protective role in colitis but the inflammation associated to colon tumor correlates with a high grade malignancy. The significant increase of MPO positive cells and of CD8+ T cells in DSS treated TG mice compared to WT mice suggests that these cells might be responsible for the extent of inflammatory response to DSS. This data is in accordance with the increase of a series of chemokines as detected by the RNAseq analysis in chronic DSS treatment (data not shown). These chemokines have the function to attract neutrophils at the site of inflammation.

Colorectal cancer is frequently associated with chronic inflammation, with the intestinal epithelial barrier playing an important protective role against the infections and injuries that cause colitis (Grivennikov *et al.* 2010; Hagerling *et al.* 2014; Schreiber *et al.* 2011). It can be supposed that the lower tumorigenic response in TG mice in the colon versus the higher tumorigenesis in the skin carcinogenesis is linked to the inflammatory components that are much more involved in the former type of carcinogenesis. The paradox of a higher inflammation rate in E933A mice but with a reduced tumor burden stimulates to search for an explanation of this difference on a potential switch in the extent/composition of the immune response. Cancer development and its response to therapy are strongly influenced by innate and adaptive immunity, which either promote or attenuate tumorigenesis and can have opposing effects on therapeutic outcome (Shalapour and Karin 2015). Many tumors express antigens that can be recognized by T lymphocytes, and analysis of the tumor microenvironment often reveals T cell infiltrates. Although CD8+ T cells are generally anti-tumorigenic, CD4+ T cell subpopulations can either promote or inhibit tumor progression (Shalapour and Karin 2015). In developing tumors both antitumorigenic and pro-tumorigenic immune and inflammatory mechanisms coexist. Certain immune and inflammatory components may be dispensable during one stage of tumorigenesis but absolutely critical in another stage. EMILIN1, likely because of its interaction with the α4β1 integrin expressed on immune cells, is protective in the initial phase but it seems absolutely critical in the final stage of colon tumorigenesis. Whether the significant increase of MPO positive cells and of CD8 cells in chronic DSS treatment has any role in the anti-tumor response in the AOM-DSS colon tumorigenesis remains to be determined.

6) MATERIAL AND METHODS

6.1) ANTIBODIES AND OTHER REAGENTS

- Rabbit polyclonal anti human EMILIN1 AS556 (produced in our laboratory)
- Anti-histidine monoclonal antibody was from Abgent (Resnova S.r.l., Rome, Italy)
- Secondary HRP-conjugated antibodies (Amersham, GE-Healthcare)
- Rabbit polyclonal Ki-67 from ABCAM
- Secondary antibodies conjugated with Alexa Fluor 488 (Invitrogen S.r.l., Milan, Italy)
- Fugene HD transfection reagent was from Roche
- Rabbit polyclonal α4 (C-terminal) from Cell Signalling
- Goat polyclonal α4 (N-terminal) from Santa Cruz
- Kit Wizard SV columns (for DNA purification from agarose gels) and Kits Wizard SV columns MINI- and MIDI- prep (for purification of DNA plasmids) were purchased from Promega
- Maxwell mouse tail purification kit was from Promega
- Trizol reagent was purchased from Invitrogen
- Dextran sulfate sodium salt (DSS) Mr ~ 40.000 from Sigma-Aldrich
- Azoxymethane (AOM) from Sigma-Aldrich

6.2) CELL CULTURES

All cell lines were obtained from ATCC and were maintained at 37°C in a humidified 5% CO_2 atmosphere. SKLMS-1, HT29, SW480 and HaCat cell lines were cultured in Complete Dulbecco's modified Eagle's medium (DMEM from Life Technologies, Inc., Gaithersburg, MD) containing 10% fetal bovine serum (FBS from Gibco, Thermo Fisher Scientific, Waltham, MA USA). Jurkat cell line was cultured in RPMI containing 10% FBS.

6.3) DNA CONSTRUCTS FOR *EMILIN1* AND *ITGA4*

To express high levels of proteins were designed constructs in which the strong viral promoter CMV is fused to the sequence coding for human *Emilin1* or *ITGA4* cDNA. For this purpose, the 2984 bp long sequence coding for the mature human EMILIN1 fused to the BM40 signal peptide was amplified via PCR with adaptor primers using as template the human pCEPu-EMILIN1 vector and cloned in the HindIII/Not sites of pBlueScript polylinker. Using the overlapping polymerase chain reaction method, a NcoI/NotI fragment of 1301 bp carrying the specific point mutation was obtained and substituted to the wild type NcoI/NotI region. The full length sequence has been then excised with HindIII and NotI and inserted in the corresponding sites of pcDNA-3 (hygro) eukariotic vector, possessing a CMV promoter and all the elements necessary for high transcription in eukaryotic cells. The resulting plasmid (and a wild type EMILIN1 containing form, as a control) was digested with AgeI and SpeI restriction enzymes and the resulting fragment was employed for transgenesis experiments for the use in transfection experiments the plasmid was simply linearized by cutting with BglII restriction enzyme.

The *ITGA4* cytoplasmic tail-deleted mutant R974 was generated by introducing a termination codon after residue R974 into che cDNA by PCR. The full-length integrin chain cloned into the Bluescript vector was used for amplification of the 1-974 region of the α4 integrin chain (α4 forward: 5’ggctcgagccatggcttgggaagcgaggcgccg3’, including a XhoI restriction site followed by a “kozak” consensus sequence at the 5’-end, and α4 reverseTM 5’ggctggcttctttaaaagataatctagagg3’ including a XbaI and XhoI restriction sites) and then subcloned in the pcDNA 3.1 vector (Invitrogen). A clone carrying the insert was sequenced and used in the subsequent experiments.

6.4) LIPOFECTION OF SK-LMS-1, HT29 AND SW480

SK-LMS-1, HT29 and SW480 cells were transiently transfected using the Fugene HD reagent method *(Promega, Madison, WI)*, according to the manufacturer's instructions. Cells were seeded into six well plates and grown to 80% confluence. 3/10 μg of the vector (*Emilin1WT*/*Emilin1*E933A/*ITGA4WT*/*ITGA4MUT*/MOCK pCDNA) were mixed 1:3 with Fugene HD reagent and taken up to 150 μl with Dulbecco's modified Eagle's medium. The mixture was incubated for 15 min at room temperature. The

lipofection mixture was added onto the cells and incubated at 37 °C for 4 hours before replacement with culture medium. 48 hours post-transfection the culture medium was replaced with Dulbecco's modified Eagle's medium with Puromycin (0.5 μg/ml) for transfectant clones selection of SKMLS1 and G418 (0.8 μg/ml) for transfectant clones selection of HT29 and SW480.

6.5) IMMUNOFLUORESCENCE STAINING OF CELLS FOR EMILIN1 AND KI-67

SK-LMS-1 were grown on cover glass slides for three days for EMILIN1 staining (24/48/72 hours for Ki-67 staining), then were fixed with 4% (w/v) paraformaldehyde, permeabilized with 0,4% Triton X-100 and blocked with 1% BSA. The appropriate primary and secondary antibodiy was use, the latter Alexa Fluor® 488 conjugate. Slides were finally mounted in Mowiol containing 2,5% (w/v) of 1,4-diazabicyclo-[2,2,2]-octane (DABCO). When needed 1 μg/ml of TO-PRO was added to label the cell nuclei. The same Ki-67 procedure was used for HT29 and SW480 grown on a coated plate but, in this case, cells were seeded in serum free medium and after 5 hours serum was added. Images were acquired with a confocal system (Leica Microsystems).

6.6) PREPARATION OF EXTRACELLULAR MATRIX EXTRACT

SK-LMS-1 were seeded into six well plates and grown to confluence. Media were discarded and cells washed with PBS; then cultures were incubated with the Lysis Solution (NP40 1% in PBS) for 10 minutes. After a wash step with PBS, 80 μl of Sample Buffer solution were added to each well and matrix was scratched and harvested.

6.7) WESTERN BLOT ANALYSIS

Matrix extracts or cells lysates were resolved in 4-20% Criterion Precast Gels (Bio-Rad Laboratories) and transferred onto Hybond-ECL nitrocellulose membranes (Amersham, GE-Healthcare). Membranes were blocked with 5% dry milk in TBS-T and probed with the appropriate antibodies and the blots were developed using ECL (Western blotting detection, Amersham Biosciences). Alternatively the ChemiDoc™ Imaging Systems

was used (BIO-RAD).

6.7.1) HRas pull down assay

The DH5alpha bacterial strain was transformed with a pGEX-2T bacterial expression vector encoding GST followed by the 2-149 N-terminal residues of human Raf-1 and induced to overexpress the protein by 0.1 mM IPTG treatment overnight at RT under shaking. This plasmid contains the RAS-binding domain (RBD) that binds only to activated Ras-GTP (gift of Channing Der, Addgene plasmid #13338). GST-Sepharose resin (GE Healthcare) was washed in cold PBS and incubated under shaking for 2h at 4°C with total bacterial proteins to allow Raf-RBD conjugation with the resin. The resin was then washed and incubated with cell lysates under shaking for 1h at 4°C. At the end of the incubation, loading buffer (0.25 M Tris-HCl pH 6.8, 10% SDS, 0.5 M dithiothreitol (DTT), 50% glycerol, 0.25% bromophenol blue) was added to each sample before protein denaturation by boiling for 10 minutes. The samples were then loaded onto 4-20% gels followed by Western Blot analysis.

6.8) FACS ANALYSIS OF:

6.8.1) Integrin expression

Cells were detached from the plate with EDTA 5mM and incubated with control IgG or the appropriate antibody in ice for at least 15 minutes or according to antibody manufacturer instructions. Cells were centrifuged to remove the antibody excess, washed twice in PBS and finally resuspended in an appropriated volume of PBS and analyzed by BD LSRFORTESSA X-20. Human α4 was detected by an anti-human CD49d (Biolegend, CA, USA) antibody conjugated with phycoerythrin (PE) whereas mouse α4 was detected with an anti-mouse integrin alpha 4 antibody [PS/2]. In addition even a home-made anti-PS2 was used.

6.8.2) Integrin sorting

We added anti-human CD49d-PE to the single cell suspension, incubated it in ice for at least 15 min, centrifuged it, discarded the supernatant, and then washed it again. We sorted a concentration of 30×10^7 with flow cytometry and collected α4 (+) cells in the flow tube.

6.8.3) Leukocytes from mice peripheral blood

Peripheral Blood samples were withdrawn (on day 8) from the cheek of mice and leukocytic cells analyzed by flow cytometry. To remove erythrocytes blood samples were treated with PharM Lyse ammonium chloride lysing reagent (BD Biosciences, San Diego, CA) for 10 minutes. Single-cell suspensions were washed with PBS 2% FCS. Cells were incubated for 20 minutes with 50 ul of 1:200 dilution of allophycocyanin-conjugated anti-mouse CD45 (clone 30-F11, eBioscience, San Diego, CA), FITC-conjugated anti-mouse GR-1 (Ly-6G, clone RB6-8C5, eBioscience), phycoerythrin-conjugated anti-mouse CD31 (clone MEC13.3, BD Biosciences), FITC-conjugated anti-mouse CD4 (L3T4, clone GK1.5, eBioscience), phycoerythrin-conjugated anti-mouse CD8a (L-2, clone 53-6.7, eBioscience), allophycocyanin-conjugated anti-mouse CD19 (clone MB19.1, eBioscience), FITC-conjugated anti-mouse B220 (clone RA3-6B2, eBioscience), phycoerythrin-conjugated anti-mouse F4/80 (clone CI:A3-1, Caltag Laboratories, Burlingame, CA), and phycoerythrin-conjugated anti-mouse CD11b (clone M1/70, BD Biosciences Pharmingen, San Jose, CA). Cells were washed twice with PBS 2% FCS (and 7-AAD - BD Biosciences - was added at a dilution of 1:10 to discriminate between viable and dead cells). Data acquisition was performed on a FACSCalibur using CellQuestPro software (BD Biosciences) and data analysis was performed using FlowJo software (Tree Star Inc.). Gates were set using negative controls and positive populations were corrected by subtraction of background and nonspecific binding of the antibody.

For setting of hierarchy myelocytes and lymphocytes subpopolations see **FIGURE 32A**.

6.8.4) Leukocytes from mice colon tissue

The same analysis used for blood was adopt for single-cell suspensions obtain from lamina propria and epithelial layer of colon mice.

Colons were opened longitudinally, cut into fine pieces, and incubated with Hanks' balanced salt solution (HBSS) containing 5 mm EDTA for 15 min at 37 °C to remove epithelial cells. Colonic pieces without epithelial cells were then incubated with PBS containing 4% fetal bovine serum (FBS), 0.5 mg ml^{-1} collagenase typeII, 1 mg ml^{-1} dispase and 50 μg ml^{-1} DNase for 20 min at 37 °C. The cells were washed twice and suspended in PBS.

6.9) PLATE COATING

Substrates, for example gC1q (whose over-expression was induced by IPTG 0,1 mM treatment of the DH5alpha bacteria previously transformed with the relative plasmids), were diluted in PBS at final concentration of 10 µg/ml and incubated on dishes overnight at 4°C. Areas of the cell culture surface potentially not coated were blocked with PBS 1% BSA for 1 hour at room temperature.

6.10) CELL ADHESION (CAFCA) ASSAY

Cell adhesion was examined using the CAFCA (Centrifugal Assay for Fluorescence-based Cell Adhesion; Spessotto *et al.* 2001), which allows for both qualitative and quantitative parameters of cell-substratum adhesion to be established. CAFCA is based on two centrifugation steps; the first one to allow a synchronized cell-substratum contact and the second one (in the reverse direction) to allow for removal of the unbound/weakly bound cells under controlled condition. The "coating solutions", composed of the ECM molecules of interest, were prepared dissolving several protein concentrations in the 0.05 M bicarbonate buffer pH 9.6, and aliquoting 50 µl in each well of the bottom CAFCA miniplates. The miniplates were incubated at 4°C for 8-16 h. After removing the coating solution from the wells, they were fill with 200 µl of 1% (w/v) BSA blocking solution and incubated at room temperature for at least 2 h. After collection of the cell suspension, cells were washed by centrifugation to remove all EDTA, and resuspended in DMEM (or another preferred medium). The cells were then incubated at 37°C for 10-20 minutes in the presence of 1-10 µM calcein (AM) (Molecular Probes Inc., Eugene, PO) to allow metabolization and subsequently fluorescent labelling. The incubation time with calcein AM may need to be extended; the optimal labelling is achieved when the cell pellet attains a yellowish color. The blocking agent were then removed from the wells, which were washed at least twice with 200 µl of the cell-adhesion medium containing PVP. The wells were fill with 200 µl of the cell-adhesion medium with 2% (v/v) India Ink. 50 µl aliquots of the labelled cells were added in each well. The bottom CAFCA miniplates were placed in the apposited bottom black holder and centrifuged at 142g for 5 min, followed by incubation 37°C for 20 min. The top CAFCA miniplate wells were fill with the same PVP-and India ink-containing medium as used for the bottom CAFCA miniplates. After

the CAFCA miniplates unit assembled, the fluorescence signal emitted by cells in wells of the top (unbound cells) and bottom (substrate-bound cells) sides were measured independently, using a microplate fluorometer (SPECTRAFluor plus, Tecan Group, Maennedorf, Switzerland). The percentage bound cells, out of the total amount of cells introduced into the system, can be calculated as: bottom fluorescence value/bottom fluorescence + top fluorescence values.

6.11) CELL-ELECTRODE IMPEDANCE, REAL-TIME CELLULAR ANALYSIS (RTCA)

Spreading and proliferation were monitored in real-time using an xCELLigence RTCA system (Acea Biosciences). This instrument uses an electrical current that is sent through gold electrodes located on the floor of each well at defined time intervals and the electrical impedances recorded. The electrical impedance readouts are expressed in terms of an arbitrary unit, the Cell Index (CI), and are displayed as kinetic curves. At each time point, the CI is calculated by Zx-Zy / Zy, where Zx is the electrical impedance of the electronic sensor in a particular well containing cells, and Zy is the background impedance of medium alone in that particular well. Prior to seeding cells, 50 µl media was added to each RTCA plate well and the plates scanned on the xCELLigence to generate a background reading.

6.11.1) The adhesion assay

The xcelligence platform is able to measure the adhesion status in real time. 50 ul of serum-free culture medium was added in each well of E-Plate 96 (Roche Applied Science) to obtain equilibrium. Cell populations/transfected cells (50,000 cells) were seeded into E-plates in serum-free growth medium. E-Plate 96 was locked in RTCA-MP device at 37 uC with 5% CO2. Impedance was measured every 5 minutes for 3 hours. The attachment rate is expressed as the change in electrical impedance at each time point with values expressed as the cell index ± SD of triplicate wells.

6.11.2) The proliferation assay

The xcelligence platform is able to measure cellular growth status in real time. As for spreading assay, 50 µl of serum-free culture medium was added in each well of E-Plate 96 (Roche Applied Science) to obtain equilibrium. Cell populations/transfected cells

(10,000 cells) were seeded into E-plates containing serum-free culture medium. E-Plate 96 was locked in RTCA-MP device at 37 °C with 5% CO2. After 5 hours serum was added to the medium at a 10% final concentration. Measured changes in electrical impedance were present as cell index that directly reflects cellular proliferation and was read automatically every 15 min and the recorded curve was shown alternatively as doubling time, the period of time required for cells to double/divide.

6.12) SOFT AGAR COLONY FORMATION ASSAY

For the bottom layer 2 ml of 0.6% agar (Sigma) dissolved in PBS and diluted in DMEM with or without 10 ug/ml gC1q were allowed to polymerize on 6 well plates. For the top layer 2 ml 0.4% agar dissolved in PBS and diluted in DMEM with or without 10 ug/ml gC1q were allowed to polymerize. Before mixing with the top agar layer, 5.0 x 10^4 HT29 cells transfected with the wild type or the deleted mutant α4 integrin chain were resuspended in DMEM containing 10% FCS and mixed with the top agar solution. Cells were allowed to grow for 12 days.

6.13) IMMUNOFLUORESCENCE STAINING OF TISSUE

Mouse tissues were excised, embedded in OCT (Kaltek, Padova, Italy), snap frozen and stored at -80°C. Cryostat sections of 7μm were air dried at room temperature and kept at -80 wrapped in aluminium foil. Before using the sections were equilibrated at room temperature, hydrated with PBS for 5 min and fixed with PBS-PFA 4% for 15 min. Then the section were permeabilized with a PBS solution containing 1% BSA, 0.4% TRITON X-100 and 2% FCS for 5 min and saturated with blocking buffer (PBS-2% FCS or NGS) and incubated with the appropriate antibodies. Images were acquired with a confocal system (Leica Microsystems).

6.14) GENOTYPING OF TRANSGENIC MICE

DNA was extracted from mice tails using Maxwell mouse tail purification kit (Promega, Italia) according to the manufacturer's protocol. PCR reaction were performed with 1:200 of total extracted DNA using goTAQ polymerase(Promega). The primers for the amplification of a specific transgene sequence and β-actin sequence were:

hEmilin1 primer

Forward (5')primer:5'-CACCTCGCAGGGCTGGCGGTG-3'

Reverse(3')primer: 5'-AGGAGCCCCAGGCCAGCTCTC-3'

Actin primers

Forward (5') primer: 5'-GAT GAC GAT ATC GCT GCG CTG GTC G-3'

Reverse (3') primer: 5'-GCC TGT GGT ACG ACC AGA GGC ATA CAG-3'

The PCR samples are run on a 1.8% agarose gel with ethidium bromide. The hEMILIN1 PCR product is identified as a band cortresponding to a length of 300 bp; the βactin PCR produce a band of 1kb.

6.15) MOUSE FIBROBLAST CULTURES ISOLATION

Newborn mice (2-3 days old) were euthanize, wash with water once, then with 70% ethanol twice. Using sterile techniques under the hood, mice tails and limbs were amputated with surgical scissors and cut on the dorsal side and along the length of the body of the mouse with a scalpel such that the skin is cut, but the internal parts of the body are intact. Carefully the skin was separated from the rest of the viscera. Skins with the dermis facing down were flatten and perfectly stretched, even at the edges, otherwise peeling is very difficult. Trypsin solution (Gibco #15050-040) was added overnight at 4°C. Using forceps the epidermis was separate from the dermis and then was added to dermis a collagenase solution (10 mg/ml H2O) for 30 mins at room temperature. The mix was filter through a sterile gauze and filtered dermis suspensions was plate in tissue culture dish containing DMEM + 10% calf serum + antibiotics and incubate in a 37°C, 5.0 CO2 incubator.

6.16) TREATMENTS *IN VIVO*

Female FVB mice (aged 8 weeks, weight 22-30 g, Jackson Laboratories, Bar Harbor, ME) used for this study were group-housed under controlled temperature (25°C) and photoperiod (12∶12-hour light–dark cycle) conditions, and given unrestricted access to standard diet and tap water (or specified drinking solution). (Mice were allowed to acclimate to these conditions for at least 7 days before inclusion in experiments)

6.16.1) DSS-induced experimental colitis

DSS 3% (molecular weight 36000–50000) was dissolved in water and treated for 7 days followed by 2 weeks consumption of waters (**FIGURE 25A**). The mice given DSS were divided into two groups and killed at day 7 of DSS administration (acute group) and at 5 weeks (chronic group). Each group consisted of five mice and was compared with control animals, which received only water. When the mice were killed the different parts of the colon were isolated for histology and for immunohistochemistry on cryostat sections. The body weight and disease activity index (DAI) were measured daily. Disease progression was assessed using DAI scoring from 0 to 4 (**FIGURE 25C**).

6.16.2) Two step-colon carcinogenesis (aom-dss) treatment

Eight week old mice were injected with 12.5 mg/kg of AOM (Sigma-Aldrich) intraperitoneally as described by Greten and colleagues. Animals were started on the first of three cycles of 3% DSS *ad libitum* (**FIGURE 30A**). Each cycle lasted 7 days and was separated by a 14-day recovery period. After the last cycle, following a 26-day recovery period, animals were sacrificed- Tumor counts and measurements were performed in a blinded fashion under a stereo-dissecting microscope. Microscopic analysis was performed for severity of inflammation and dysplasia on (H&E) stained "Swiss rolled" colons by a pathologist. All *in vivo* procedures were carried out in accordance with protocols approved by Animal Care and Use Committee. Body weight was assessed at least 3 days per week throughout the course of the experiment.

6.17) HISTOPATOLOGY AND IMMUNOHISTOCHEMISTRY

6.17.1) Samples processing

1 cm of the distal colon was embedded in OCT and 7-µm sections were fixed in 10% formalin.

5 replicates from each case were analyzed.

Histopathology: sections were stained with hematoxylin and eosin (H&E) and then examined with a light microscope for the detection and quantification of histological lesions.

Immunohistochemistry: sections immunostained with the following primary antibodies (tab. 1):

Tab. 1 – Primary antibodies applied.

Primary Ab	**Clonality**	**Identification of**
CD45R/B220	Rat mon	B cells
CD3 epsilon	Goat poly	T cells
Myeloperoxidase (MPO)	Rabbit poly	Granulocytes
Ki67	Rabbit mon	Proliferating cells

Sections were incubated with biotinylated secondary antibody (rabbit anti-rat; rabbit anti-goat; goat anti-rabbit). Sections were labelled by the avidin-biotin-peroxidase (ABC) procedure with a commercial immunoperoxidase kit. The immunoreaction was visualized with 3,3'-diaminobenzidine (DAB) substrate and sections were counterstained with Mayer's hematoxylin.

6.17.2) Examination procedures

Evaluation (histopathology): histopathology evaluation was made in a blind fashion, ie without knowledge of the treatment group. The following findings have been detected and scored:

- Epithelial damage: loss of the epithelial layer of the enteric mucosa. This finding was scored as follow:
  - 0 = absence of epithelial damage
  - 1 = moderate epithelial damage
  - 2 = severe epithelial damage
- Lamina propria (LP) infiltrate: presence of infiltrating inflammatory cells within lamina propria. This finding was scored as follow:
  - 0 = absence of infiltrating cells
  - 1 = moderate presence of infiltrating cells
  - 2 = severe presence of infiltrating cells
- Small/large follicles: presence of lymphoid follicles: the number of small and large lymphoid follicle was reported. Lymphoid follicles were considered small when composed of < 100 cells; follicles were considered large when composed of 100 or more cells.

Evaluation (immunohistochemistry): immunohistochemical evaluation was made in a blind fashion, ie without knowledge of the treatment group.

- Immunostainings for inflammatory cells (CD45R/B220, CD3 epsilon, MPO) were scored counting the number of positive cells as follows:
  0 = 0
  1 = 1 to 5 cells
  2 = 6 to 25 cells
  3 = 25 to 125 cells
  4 = > 125 cells

- Immunostaining for KI67 was evaluated and two scores were applied as follows:

% of mucosa: percentage of mucosa with positive intestinal glands. Note: in normal mucosa this parameter is 100 or near 100 (all/most of the glands have cells that are proliferating).

% of gland: percentage of the gland positively stained. Note: in normal mucosa this parameter is 50 or near 50 (half part of each gland is stained, namely the deeper part).

6.18) ENDOSCOPIC ASSESSMENT OF COLITIS

Direct visualization of DSS-induced colonic mucosal damage *in vivo* was performed using the Coloview (Karl Storz Veterinary Endoscopy, Tuttlingen, Germany). Mice were supplied with food and water until the endoscopy was performed. Mice were anesthetized with 1.5 to 2% isoflurane and 3 cm of the colon proximal to the anus was visualized after inflation of the colon with air. The endoscopic damage score was determined using a previously described scoring method MEICS: assessment of colon translucency (0–3 points), presence of fibrin attached to the bowel wall (0–3 points), granular aspect of the mucosa (0–3 points), morphology of the vascular pattern (0–3 points), and stool characteristic (normal to diarrhea; 0–3 points).

7) REFERENCES

- Arnaout MA, Goodman SL, Xiong JP. Coming to grips with integrin binding to ligands. Curr Opin Cell Biol. 2002 Oct;14(5):641-51. Review. PubMed PMID: 12231361.
- Arnaout MA, Goodman SL, Xiong JP. Structure and mechanics of integrin-based cell adhesion. Curr Opin Cell Biol. 2007 Oct;19(5):495-507. Review. PubMed PMID: 17928215; PubMed Central PMCID: PMC2443699.
- Ausch C, Kim YH, Tsuchiya KD, Dzieciatkowski S, Washington MK, Paraskeva C, Radich J, Grady WM. Comparative analysis of PCR-based biomarker assay methods for colorectal polyp detection from fecal DNA. Clin Chem. 2009 Aug;55(8):1559-63. Doi: 10.1373/clinchem.2008.122937. PubMed PMID: 19541867.
- Barczyk M, Carracedo S, Gullberg D. Integrins. Cell Tissue Res. 2010 Jan;339(1):269-80. doi: 10.1007/s00441-009-0834-6. Review. PubMed PMID: 19693543; PubMed Central PMCID: PMC2784866.
- Bissell MJ, Kenny PA, Radisky DC. Microenvironmental regulators of tissue structure and function also regulate tumor induction and progression: the role of extracellular matrix and its degrading enzymes. Cold Spring Harb Symp Quant Biol. 2005;70:343-56. PubMed PMID: 16869771; PubMed Central PMCID: PMC3004779.
- Bjursten M, Bland PW, Willén R, Hörnquist EH. Long-term treatment with anti-alpha 4 integrin antibodies aggravates colitis in G alpha i2-deficient mice. Eur J Immunol. 2005 Aug;35(8):2274-83. PubMed PMID: 16052630.
- Boehmler AM, Drost A, Jaggy L, Seitz G, Wiesner T, Denzlinger C, Kanz L, Möhle R. The CysLT1 ligand leukotriene D4 supports alpha4beta1- and alpha5beta1-mediated adhesion and proliferation of CD34+ hematopoietic progenitor cells. J Immunol. 2009 Jun 1;182(11):6789-98. doi: 10.4049/jimmunol.0801525. PubMed PMID: 19454674.
- Braghetta P, Ferrari A, De Gemmis P, Zanetti M, Volpin D, Bonaldo P, Bressan GM. Overlapping, complementary and site-specific expression pattern of genes of the EMILIN/Multimerin family. Matrix Biol. 2004 Jan;22(7):549-56. PubMed PMID: 14996434.
- Bressan GM, Daga-Gordini D, Colombatti A, Castellani I, Marigo V, Volpin D. Emilin, a component of elastic fibers preferentially located at the elastin-microfibrils interface. J Cell Biol. 1993 Apr;121(1):201-12. PubMed PMID: 8458869; PubMed Central PMCID: PMC2119774.
- Campbell ID. Studies of focal adhesion assembly. Biochem Soc Trans. 2008 Apr;36(Pt 2):263-6. doi: 10.1042/BST0360263. Review. PubMed PMID: 18363570.
- Casasnovas JM, Stehle T, Liu JH, Wang JH, Springer TA. A dimeric crystal structure for the N-terminal two domains of intercellular adhesion molecule-1. Proc Natl Acad Sci U S A. 1998 Apr 14;95(8):4134-9. PubMed PMID: 9539702; PubMed Central PMCID: PMC22454.
- Cherny RC, Honan MA, Thiagarajan P. Site-directed mutagenesis of the arginine-glycine-aspartic acid in vitronectin abolishes cell adhesion. J Biol Chem. 1993 May 5;268(13):9725-9. PubMed PMID: 7683657.
- Christian S, Ahorn H, Novatchkova M, Garin-Chesa P, Park JE, Weber G, Eisenhaber F, Rettig WJ, Lenter MC. Molecular cloning and characterization of EndoGlyx-1, an EMILIN-like multisubunit glycoprotein of vascular

endothelium. J Biol Chem. 2001 Dec 21;276(51):48588-95. PubMed PMID: 11559704.
- Clark EA, Brugge JS. Integrins and signal transduction pathways: the road taken. Science. 1995 Apr 14;268(5208):233-9. Review. PubMed PMID: 7716514.
- Clark K, Newham P, Burrows L, Askari JA, Humphries MJ. Production of recombinant soluble human integrin alpha4beta1. FEBS Lett. 2000 Apr 14;471(2-3):182-6. PubMed PMID: 10767419.
- Clements JM, Newham P, Shepherd M, Gilbert R, Dudgeon TJ, Needham LA, Edwards RM, Berry L, Brass A, Humphries MJ. Identification of a key integrin-binding sequence in VCAM-1 homologous to the LDV active site in fibronectin. J Cell Sci. 1994 Aug;107 (Pt 8):2127-35. PubMed PMID: 7527054.
- Colombatti A, Bressan GM, Castellani I, Volpin D. Glycoprotein 115, a glycoprotein isolated from chick blood vessels, is widely distributed in connective tissue. J Cell Biol. 1985 Jan;100(1):18-26. PubMed PMID: 3880750; PubMed Central PMCID: PMC2113488.
- Colombatti A, Doliana R, Bot S, Canton A, Mongiat M, Mungiguerra G, Paron-Cilli S, Spessotto P. The EMILIN protein family. Matrix Biol. 2000 Aug;19(4):289-301. Review. PubMed PMID: 10963989.
- Colombatti A, Spessotto P, Doliana R, Mongiat M, Bressan GM, Esposito G. The EMILIN/Multimerin family. Front Immunol. 2012 Jan 6;2:93. doi: 10.3389/fimmu.2011.00093. PubMed PMID: 22566882; PubMed Central PMCID: PMC3342094.
- Conway D, Cohen JA. Combination therapy in multiple sclerosis. Lancet Neurol. 2010 Mar;9(3):299-308. doi: 10.1016/S1474-4422(10)70007-7. Review. PubMed PMID: 20170843.
- Cox TR, Erler JT. Remodeling and homeostasis of the extracellular matrix: implications for fibrotic diseases and cancer. Dis Model Mech. 2011 Mar;4(2):165-78. Doi: 10.1242/dmm.004077. PubMed PMID: 21324931; PubMed Central PMCID: PMC3046088.
- Cukierman E, Bassi DE. Physico-mechanical aspects of extracellular matrix influences on tumorigenic behaviors. Semin Cancer Biol. 2010 Jun;20(3):139-45. Doi: 10.1016/j.semcancer.2010.04.004. Review. PubMed PMID: 20452434; PubMed Central PMCID: PMC2941524.
- Danussi C, Del Bel Belluz L, Pivetta E, Modica TM, Muro A, Wassermann B, Doliana R, Sabatelli P, Colombatti A, Spessotto P. EMILIN1/α9β1 integrin interaction is crucial in lymphatic valve formation and maintenance. Mol Cell Biol. 2013 Nov;33(22):4381-94. doi: 10.1128/MCB.00872-13. PubMed PMID: 24019067; PubMed Central PMCID: PMC3838180.
- Danussi C, Petrucco A, Wassermann B, Pivetta E, Modica TM, Del Bel Belluz L, Colombatti A, Spessotto P. EMILIN1-α4/α9 integrin interaction inhibits dermal fibroblast and keratinocyte proliferation. J Cell Biol. 2011 Oct 3;195(1):131-45. doi: 10.1083/jcb.201008013. PubMed PMID: 21949412; PubMed Central PMCID: PMC3187715.
- Danussi C, Spessotto P, Petrucco A, Wassermann B, Sabatelli P, Montesi M, Doliana R, Bressan GM, Colombatti A. Emilin1 deficiency causes structural and functional defects of lymphatic vasculature. Mol Cell Biol. 2008 Jun;28(12):4026-39. doi: 10.1128/MCB.02062-07. PubMed PMID: 18411305; PubMed Central PMCID: PMC2423131.
- Desilva S, Kaplan G, Panaccione R. Sequential therapies for Crohn's disease:

optimizing conventional and biologic strategies. Rev Gastroenterol Disord. 2008 Spring;8(2):109-16. Review. PubMed PMID: 18641593.

- Di Cristofano A, Pesce B, Cordon-Cardo C, Pandolfi PP. Pten is essential for embryonic development and tumour suppression. Nat Genet. 1998 Aug;19(4):348-55. PubMed PMID: 9697695.
- Doliana R, Bot S, Mungiguerra G, Canton A, Cilli SP, Colombatti A. Isolation and characterization of EMILIN-2, a new component of the growing EMILINs family and a member of the EMI domain-containing superfamily. J Biol Chem. 2001 Apr 13;276(15):12003-11. PubMed PMID: 11278945.
- Doliana R, Mongiat M, Bucciotti F, Giacomello E, Deutzmann R, Volpin D, Bressan GM, Colombatti A. EMILIN, a component of the elastic fiber and a new member of the C1q/tumor necrosis factor superfamily of proteins. J Biol Chem. 1999 Jun 11;274(24):16773-81. PubMed PMID: 10358019.
- Gerecke C, Scholtka B, Löwenstein Y, Fait I, Gottschalk U, Rogoll D, Melcher R, Kleuser B. Hypermethylation of ITGA4, TFPI2 and VIMENTIN promoters is increased in inflamed colon tissue: putative risk markers for colitis-associated cancer. J Cancer Res Clin Oncol. 2015 Dec;141(12):2097-107. Doi: 10.1007/s00432-015-1972-8. PubMed PMID: 25902909.
- Gilcrease MZ. Integrin signaling in epithelial cells. Cancer Lett. 2007 Mar 8;247(1):1-25. Review. PubMed PMID: 16725254.
- Gillberg L, Berg S, de Verdier PJ, Lindbom L, Werr J, Hellström PM. Effective treatment of mouse experimental colitis by alpha 2 integrin antibody: comparison with alpha 4 antibody and conventional therapy. Acta Physiol (Oxf). 2013 Feb;207(2):326-36. Doi: 10.1111/apha.12017. PubMed PMID: 23009282.
- Grivennikov SI, Greten FR, Karin M. Immunity, inflammation, and cancer. Cell. 2010 Mar 19;140(6):883-99. doi: 10.1016/j.cell.2010.01.025. Review. PubMed PMID: 20303878; PubMed Central PMCID: PMC2866629.
- Hagerling C, Casbon AJ, Werb Z. Balancing the innate immune system in tumor development. Trends Cell Biol. 2015 Apr;25(4):214-20. Doi: 10.1016/j.tcb.2014.11.001. Review. PubMed PMID: 25444276; PubMed Central PMCID: PMC4380818.
- Hamann A, Andrew DP, Jablonski-Westrich D, Holzmann B, Butcher EC. Role of alpha 4-integrins in lymphocyte homing to mucosal tissues in vivo. J Immunol. 1994 Apr 1;152(7):3282-93. PubMed PMID: 7511642.
- Hayward CP, Hassell JA, Denomme GA, Rachubinski RA, Brown C, Kelton JG. The cDNA sequence of human endothelial cell multimerin. A unique protein with RGDS, coiled-coil, and epidermal growth factor-like domains and a carboxyl terminus similar to the globular domain of complement C1q and collagens type VIII and X. J Biol Chem. 1995 Aug 4;270(31):18246-51. PubMed PMID: 7629143.
- Hayward CP, Smith JW, Horsewood P, Warkentin TE, Kelton JG. p-155, a multimeric platelet protein that is expressed on activated platelets. J Biol Chem. 1991 Apr 15;266(11):7114-20. PubMed PMID: 2016319.
- Holzmann B, Gosslar U, Bittner M. alpha 4 integrins and tumor metastasis. Curr Top Microbiol Immunol. 1998;231:125-41. Review. PubMed PMID: 9479864.
- Hsia DA, Lim ST, Bernard-Trifilo JA, Mitra SK, Tanaka S, den Hertog J, Streblow DN, Ilic D, Ginsberg MH, Schlaepfer DD. Integrin alpha4beta1 promotes focal adhesion kinase-independent cell motility via alpha4 cytoplasmic domain-specific activation of c-Src. Mol Cell Biol. 2005 Nov;25(21):9700-12. PubMed PMID: 16227616; PubMed Central PMCID: PMC1265817.

- Humphries JD, Byron A, Humphries MJ. Integrin ligands at a glance. J Cell Sci. 2006 Oct 1;119(Pt 19):3901-3. Review. PubMed PMID: 16988024; PubMed Central PMCID: PMC3380273.
- Humphries MJ. The molecular basis and specificity of integrin-ligand interactions. J Cell Sci. 1990 Dec;97 (Pt 4):585-92. Review. PubMed PMID: 2077034.
- Hynes RO. The extracellular matrix: not just pretty fibrils. Science. 2009 Nov 27;326(5957):1216-9. doi: 10.1126/science.1176009. Review. PubMed PMID: 19965464; PubMed Central PMCID: PMC3536535.
- Komoriya A, Green LJ, Mervic M, Yamada SS, Yamada KM, Humphries MJ. The minimal essential sequence for a major cell type-specific adhesion site (CS1) within the alternatively spliced type III connecting segment domain of fibronectin is leucine-aspartic acid-valine. J Biol Chem. 1991 Aug 15;266(23):15075-9. PubMed PMID: 1869542.
- Lakatos PL, Burisch J. Environment and invironment in IBDs: partners in crime. Gut. 2015 Jul;64(7):1009-10. doi: 10.1136/gutjnl-2014-308460. PubMed PMID: 25336112.
- Leahy DJ, Aukhil I, Erickson HP. 2.0 A crystal structure of a four-domain segment of human fibronectin encompassing the RGD loop and synergy region. Cell. 1996 Jan 12;84(1):155-64. PubMed PMID: 8548820.
- Legate KR, Wickström SA, Fässler R. Genetic and cell biological analysis of integrin outside-in signaling. Genes Dev. 2009 Feb 15;23(4):397-418. doi: 10.1101/gad.1758709. Review. PubMed PMID: 19240129.
- Leimeister C, Steidl C, Schumacher N, Erhard S, Gessler M. Developmental expression and biochemical characterization of Emu family members. Dev Biol. 2002 Sep 15;249(2):204-18. PubMed PMID: 12221002.
- Levental KR, Yu H, Kass L, Lakins JN, Egeblad M, Erler JT, Fong SF, Csiszar K, Giaccia A, Weninger W, Yamauchi M, Gasser DL, Weaver VM. Matrix crosslinking forces tumor progression by enhancing integrin signaling. Cell. 2009 Nov 25;139(5):891-906. doi: 10.1016/j.cell.2009.10.027. PubMed PMID: 19931152; PubMed Central PMCID: PMC2788004.
- Li H, Fan X, Houghton J. Tumor microenvironment: the role of the tumor stroma in cancer. J Cell Biochem. 2007 Jul 1;101(4):805-15. Review. PubMed PMID: 17226777.
- Makarem R, Newham P, Askari JA, Green LJ, Clements J, Edwards M, Humphries MJ, Mould AP. Competitive binding of vascular cell adhesion molecule-1 and the HepII/IIICS domain of fibronectin to the integrin alpha 4 beta 1. J Biol Chem. 1994 Feb 11;269(6):4005-11. PubMed PMID: 7508437.
- Marastoni S, Ligresti G, Lorenzon E, Colombatti A, Mongiat M. Extracellular matrix: a matter of life and death. Connect Tissue Res. 2008;49(3):203-6. doi: 10.1080/03008200802143190. Review. PubMed PMID: 18661343.
- Masumoto A, Hemler ME. Multiple activation states of VLA-4. Mechanistic differences between adhesion to CS1/fibronectin and to vascular cell adhesion molecule-1. J Biol Chem. 1993 Jan 5;268(1):228-34. PubMed PMID: 7677996.
- Modica TM, Maiorani O, Sartori G, Pivetta E, Doliana R, Capuano A, Colombatti A, Spessotto P. The extracellular matrix protein EMILIN1 silences the RAS-ERK pathway via α4β1 integrin and decreases tumor cell growth. Oncotarget. 2017 Feb 3. doi: 10.18632/oncotarget.15067. PubMed PMID: 28177903.
- Michishita M, Videm V, Arnaout MA. A novel divalent cation-binding site in the

A domain of the beta 2 integrin CR3 (CD11b/CD18) is essential for ligand binding. Cell. 1993 Mar 26;72(6):857-67. PubMed PMID: 8458080.

- Moreno-Layseca P, Streuli CH. Signalling pathways linking integrins with cell cycle progression. Matrix Biol. 2014 Feb;34:144-53. Doi: 10.1016/j.matbio.2013.10.011. Review. PubMed PMID: 24184828.
- Müller EJ, Williamson L, Kolly C, Suter MM. Outside-in signaling through integrins and cadherins: a central mechanism to control epidermal growth and differentiation? J Invest Dermatol. 2008 Mar;128(3):501-16. Doi: 10.1038/sj.jid.5701248. Review. PubMed PMID: 18268536.
- Petit V, Thiery JP. Focal adhesions: structure and dynamics. Biol Cell. 2000 Oct;92(7):477-94. Review. PubMed PMID: 11229600.
- Pierschbacher MD, Ruoslahti E. Variants of the cell recognition site of fibronectin that retain attachment-promoting activity. Proc Natl Acad Sci U S A. 1984 Oct;81(19):5985-8. PubMed PMID: 6237366; PubMed Central PMCID: PMC391843.
- Pinco KA, He W, Yang JT. alpha4beta1 integrin regulates lamellipodia protrusion via a focal complex/focal adhesion-independent mechanism. Mol Biol Cell. 2002 Sep;13(9):3203-17. PubMed PMID: 12221126; PubMed Central PMCID: PMC124153.
- Provenzano PP, Keely PJ. Mechanical signaling through the cytoskeleton regulates cell proliferation by coordinated focal adhesion and Rho GTPase signaling. J Cell Sci. 2011 Apr 15;124(Pt 8):1195-205. doi: 10.1242/jcs.067009. PubMed PMID: 21444750; PubMed Central PMCID: PMC3065381.
- Risques RA, Lai LA, Himmetoglu C, Ebaee A, Li L, Feng Z, Bronner MP, Al-Lahham B, Kowdley KV, Lindor KD, Rabinovitch PS, Brentnall TA. Ulcerative colitis-associated colorectal cancer arises in a field of short telomeres, senescence, and inflammation. Cancer Res. 2011 Mar 1;71(5):1669-79. doi: 10.1158/0008-5472.CAN-10-1966. PubMed PMID: 21363920; PubMed Central PMCID: PMC3077943.
- Ruoslahti E, Pierschbacher MD. New perspectives in cell adhesion: RGD and integrins. Science. 1987 Oct 23;238(4826):491-7. Review. PubMed PMID: 2821619.
- Ruoslahti E. Fibronectin and its integrin receptors in cancer. Adv Cancer Res. 1999;76:1-20. Review. PubMed PMID: 10218097.
- Sanz-Moncasi MP, Garin-Chesa P, Stockert E, Jaffe EA, Old LJ, Rettig WJ. Identification of a high molecular weight endothelial cell surface glycoprotein, endoGlyx-1, in normal and tumor blood vessels. Lab Invest. 1994 Sep;71(3):366-73. PubMed PMID: 7933987.
- Schindler EM, Hindes A, Gribben EL, Burns CJ, Yin Y, Lin MH, Owen RJ, Longmore GD, Kissling GE, Arthur JS, Efimova T. p38delta Mitogen-activated protein kinase is essential for skin tumor development in mice. Cancer Res. 2009 Jun 1;69(11):4648-55. doi 10.1158/0008-5472.CAN-08-4455. PubMed PMID: 19458068.
- Schlaepfer DD, Hanks SK, Hunter T, van der Geer P. Integrin-mediated signal transduction linked to Ras pathway by GRB2 binding to focal adhesion kinase. Nature. 1994 Dec 22-29;372(6508):786-91. PubMed PMID: 7997267.
- Schreiber RD, Old LJ, Smyth MJ. Cancer immunoediting: integrating immunity's roles in cancer suppression and promotion. Science. 2011 Mar 25;331(6024):1565-70. doi: 10.1126/science.1203486. Review. PubMed PMID: 21436444.

- Segrelles C, Ruiz S, Perez P, Murga C, Santos M, Budunova IV, Martínez J, Larcher F, Slaga TJ, Gutkind JS, Jorcano JL, Paramio JM. Functional roles of Akt signaling in mouse skin tumorigenesis. Oncogene. 2002 Jan 3;21(1):53-64. PubMed PMID: 11791176.
- Shalapour S, Karin M. Immunity, inflammation, and cancer: an eternal fight between good and evil. J Clin Invest. 2015 Sep;125(9):3347-55. Doi: 10.1172/JCI80007. Review. PubMed PMID: 26325032; PubMed Central PMCID: PMC4588298.
- Spessotto P, Bulla R, Danussi C, Radillo O, Cervi M, Monami G, Bossi F, Tedesco F, Doliana R, Colombatti A. EMILIN1 represents a major stromal element determining human trophoblast invasion of the uterine wall. J Cell Sci. 2006 Nov 1;119(Pt 21):4574-84. PubMed PMID: 17074837.
- Spessotto P, Cervi M, Mucignat MT, Mungiguerra G, Sartoretto I, Doliana R, Colombatti A. beta 1 Integrin-dependent cell adhesion to EMILIN-1 is mediated by the gC1q domain. J Biol Chem. 2003 Feb 21;278(8):6160-7. PubMed PMID: 12456677.
- Stephens PE, Ortlepp S, Perkins VC, Robinson MK, Kirby H. Expression of a soluble functional form of the integrin alpha4beta1 in mammalian cells. Cell Adhes Commun. 2000 May;7(5):377-90. PubMed PMID: 10830617.
- Streuli CH. Integrins and cell-fate determination. J Cell Sci. 2009 Jan 15;122(Pt 2):171-7. doi: 10.1242/jcs.018945. Review. PubMed PMID: 19118209; PubMed Central PMCID: PMC2714415.
- Suzuki A, Itami S, Ohishi M, Hamada K, Inoue T, Komazawa N, Senoo H, Sasaki T, Takeda J, Manabe M, Mak TW, Nakano T. Keratinocyte-specific Pten deficiency results in epidermal hyperplasia, accelerated hair follicle morphogenesis and tumor formation. Cancer Res. 2003 Feb 1;63(3):674-81. PubMed PMID: 12566313.
- Verdone G, Colebrooke SA, Boyd J, Viglino P, Corazza A, Doliana R, Mungiguerra G, Colombatti A, Esposito G, Campbell ID. Sequence-specific backbone NMR assignments for the C-terminal globular domain of EMILIN-1. J Biomol NMR. 2004 May;29(1):91-2. PubMed PMID: 15017143.
- Verdone G, Corazza A, Colebrooke SA, Cicero D, Eliseo T, Boyd J, Doliana R, Fogolari F, Viglino P, Colombatti A, Campbell ID, Esposito G. NMR-based homology model for the solution structure of the C-terminal globular domain of EMILIN1. J Biomol NMR. 2009 Feb;43(2):79-96. doi: 10.1007/s10858-008-9290-y. PubMed PMID: 19023665.
- Verdone G, Doliana R, Corazza A, Colebrooke SA, Spessotto P, Bot S, Bucciotti F, Capuano A, Silvestri A, Viglino P, Campbell ID, Colombatti A, Esposito G. The solution structure of EMILIN1 globular C1q domain reveals a disordered insertion necessary for interaction with the alpha4beta1 integrin. J Biol Chem. 2008 Jul 4;283(27):18947-56. doi: 10.1074/jbc.M801085200. PubMed PMID: 18463100.
- Vermeulen L, Morrissey E, van der Heijden M, Nicholson AM, Sottoriva A, Buczacki S, Kemp R, Tavaré S, Winton DJ. Defining stem cell dynamics in models of intestinal tumor initiation. Science. 2013 Nov 22;342(6161):995-8. doi: 10.1126/science.1243148. PubMed PMID: 24264992.
- Vesely MD, Kershaw MH, Schreiber RD, Smyth MJ. Natural innate and adaptive immunity to cancer. Annu Rev Immunol. 2011;29:235-71. doi: 10.1146/annurev-immunol-031210-101324. Review. PubMed PMID: 21219185.
- Walker JL, Assoian RK. Integrin-dependent signal transduction regulating cyclin

D1 expression and G1 phase cell cycle progression. Cancer Metastasis Rev. 2005 Sep;24(3):383-93. Review. PubMed PMID: 16258726.

- Wang JH, Pepinsky RB, Stehle T, Liu JH, Karpusas M, Browning B, Osborn L. The crystal structure of an N-terminal two-domain fragment of vascular cell adhesion molecule 1 (VCAM-1): a cyclic peptide based on the domain 1 C-D loop can inhibit VCAM-1-alpha 4 integrin interaction. Proc Natl Acad Sci U S A. 1995 Jun 6;92(12):5714-8. PubMed PMID: 7539925; PubMed Central PMCID: PMC41767.
- Williams AF, Barclay AN. The immunoglobulin superfamily--domains for cell surface recognition. Annu Rev Immunol. 1988;6:381-405. Review. PubMed PMID: 3289571.
- Yamada KM. Adhesive recognition sequences. J Biol Chem. 1991 Jul 15;266(20):12809-12. Review. PubMed PMID: 2071570.
- Yang GX, Hagmann WK. VLA-4 antagonists: potent inhibitors of lymphocyte migration. Med Res Rev. 2003 May;23(3):369-92. Review. PubMed PMID: 12647315.
- You TJ, Maxwell DS, Kogan TP, Chen Q, Li J, Kassir J, Holland GW, Dixon RA. A 3D structure model of integrin alpha 4 beta 1 complex: I. Construction of a homology model of beta 1 and ligand binding analysis. Biophys J. 2002 Jan;82(1 Pt 1):447-57. PubMed PMID: 11751331; PubMed Central PMCID: PMC1302484.
- Yusuf-Makagiansar H, Anderson ME, Yakovleva TV, Murray JS, Siahaan TJ. Inhibition of LFA-1/ICAM-1 and VLA-4/VCAM-1 as a therapeutic approach to inflammation an autoimmune diseases. Med Res Rev. 2002 Mar;22(2):146-67. Review. PubMed PMID: 11857637.
- Zacchigna L, Vecchione C, Notte A, Cordenonsi M, Dupont S, Maretto S, Cifelli G, Ferrari A, Maffei A, Fabbro C, Braghetta P, Marino G, Selvetella G, Aretini A, Colonnese C, Bettarini U, Russo G, Soligo S, Adorno M, Bonaldo P, Volpin D, Piccolo S, Lembo G, Bressan GM. Emilin1 links TGF-beta maturation to blood pressure homeostasis. Cell. 2006 Mar 10;124(5):929-42. PubMed PMID: 16530041.
- Zanetti M, Braghetta P, Sabatelli P, Mura I, Doliana R, Colombatti A, Volpin D, Bonaldo P, Bressan GM. EMILIN-1 deficiency induces elastogenesis and vascular cell defects. Mol Cell Biol. 2004 Jan;24(2):638-50. PubMed PMID: 14701737; PubMed Central PMCID: PMC343785.
- Zhang W, Huang P. Cancer-stromal interactions: role in cell survival, metabolism and drug sensitivity. Cancer Biol Ther. 2011 Jan 15;11(2):150-6. Review. PubMed PMID: 21191189; PubMed Central PMCID: PMC3230306.
- Zhang X, Song YF, Lu HN, Wang DP, Zhang XS, Huang SL, Sun BL, Huang ZG. Combined detection of plasma GATA5 and SFRP2 methylation is a valid noninvasive biomarker for colorectal cancer and adenomas. World J Gastroenterol. 2015 Mar 7;21(9):2629-37. doi: 10.3748/wjg.v21.i9.2629. PubMed PMID: 25759530; PubMed Central PMCID: PMC4351212.
- Zouq NK, Keeble JA, Lindsay J, Valentijn AJ, Zhang L, Mills D, Turner CE, Streuli CH, Gilmore AP. FAK engages multiple pathways to maintain survival of fibroblasts and epithelia: differential roles for paxillin and p130Cas. J Cell Sci. 2009 Feb 1;122(Pt 3):357-67. doi 10.1242/jcs.030478. PubMed PMID: 19126677; PubMed Central PMCID: PMC2724727.

8) PUBLICATIONS

Modica TM, Maiorani O, **Sartori G**, Pivetta E, Doliana R, Capuano A, Colombatti A, Spessotto P. The extracellular matrix protein EMILIN1 silences the RAS-ERK pathway via α4β1 integrin and decreases tumor cell growth. Oncotarget. 2017 Feb 3. doi: 10.18632/oncotarget.15067. PubMed PMID: 28177903.

9) ACKNOWLEDGEMENTS

I would like to thank all the colleagues belonging to the Experimental Oncology 2 of CRO Aviano National Cancer Institute for the fun and support and in particular:

Elisa Modica and Orlando Maiorani for the *in vitro* part.
Alessandra Capuano for the *in vivo* part.
Eva Andreuzzi for the FACS analysis.

Eliana Pivetta and Bruna Wasserman for helpful suggestions and advises and also for their time and extreme patience.

Paola Spessotto, Roberto Doliana and Maurizio Mongiat for offering me the opportunities to join their groups and for helping me to develop the present study.

Special thanks to Alfonso Colomabatti for intellectual contributions to my development as a scientist. His guidance helped me in all the time of research and writing of this thesis.